Shootin1a dephosphorylation by protein phosphatase 1 for netrin-1–induced axon guidance

Kaewkascholkul Napol

Nara Institute of Science and Technology
Graduate School of Science and Technology

Systems Neurobiology and Medicine
(Naoyuki Inagaki)

2021/09/13

Introduction

Axon guidance toward appropriate synaptic partners is critical for the formation of neuronal networks. Guidance cues are presented bound to extracellular matrix to form haptotactic gradients or secreted to form soluble chemotactic gradients. The growth cone, a highly dynamic structure at the end of the extending axon, senses the guidance cues via transmembrane receptors (Kolodkin and Tessier-Lavigne, 2011). Attractive and repulsive guidance cues interact with receptors on the axon surface and trigger signaling pathway for the growth cone turning (Lowery and Vactor, 2009).

Netrins are a family of secreted proteins that control axon outgrowth and guidance in multiple vertebrate and invertebrates species (Barallobre et al., 2005). Netrin-1, the most studied member of the family, is a bifunctional molecule that attracts and repels the axon direction. In vertebrates, netrin-1 was first shown to attract commissural axons in developing spinal cord toward the ventral midline (Kennedy et al., 1994; Serafini et al., 1994). Two families of netrin-1 receptors have been identified: deleted in colorectal cancer (DCC) family and UNC-5 family (Ackerman et al., 1997; Keino-Masu et al., 1996). DCC is involved in growth cones attraction induced by netrin-1 whereas the repulsion by netrin-1 is mediated by UNC-5 family. Netrin-1 and DCC are required for midline crossing in many central nervous system axons (Kennedy et al., 1994; Serafini et al., 1996). Mice deficiency in netrin-1 or DCC show loss of axon projection and guidance in the ventral spinal commissure and forebrain commissure (Bin et al., 2015; Fazeli et al., 1997; Serafini et al., 1996).

Shootin1a is a brain-specific protein involved in neuronal symmetry breaking, polarity formation, signal–mediated axon outgrowth, axonal transport and axon guidance (Baba et al., 2018; Katsuno et al., 2015; Kubo et al., 2015; Shimada et al., 2008; Toriyama et al., 2006, 2010, 2013). Recently, our group reported that shootin1a–mediated clutch coupling and actin polymerization are required for the force generation in spine enlargement (Kastian et al., 2021). At the leading edge of axonal growth cones, shootin1a mechanically couples actin filament (F-actin) retrograde flow (Forscher and Smith, 1988; Katoh et al., 1999) and adhesive substrate

through an actin-binding protein cortactin (Kubo et al., 2015) and cell adhesion molecule L1-CAM (Baba et al., 2018; Shimada et al., 2008). Netrin-1 induces shootin1a phosphorylation at Ser101 and Ser249 through p21-activated kinase 1 (Pak1) (Toriyama et al., 2013). In addition, phosphorylation of shootin1a enhances the bindings of shootin1a to cortactin and L1-CAM, resulting in the promotion of traction force for axon outgrowth and guidance (Baba et al., 2018; Kubo et al., 2015).

Mice lacking shootin1a display abnormal projection of forebrain commissural axons, a phenotype similar to that of *Netrin-1* knock out mice (Baba et al., 2018). Extracellular gradients of netrin-1 induce attractive axon turning *in vitro* (Bhattacharjee et al., 2010; Hong et al., 1999; Kennedy et al., 1994). An extracellular gradient of guidance cue induces the asymmetric distribution of proteins including cytoskeletal proteins and receptors in the growth cone (Bouzigues et al., 2007; Lin and Forscher, 1993; Yao et al., 2006). The shallow gradient of netrin-1 concentration can induce highly polarized phosphorylation of shootin1a within growth cones, through a signaling pathway including DCC, Rac1/CDC42 and Pak1 (Figure 1). The polarized phosphorylation of shootin1a locally promotes shootin1a–L1-CAM and shootin1a–cortactin interactions. These spatially different interactions of shootin1a and binding partners induce directional traction force toward the netrin-1 source, thereby leading to a decision of the migratory direction (Figure 1). Shootin1a phosphorylation within growth cones is required for netrin-1–induced axon turning (Baba et al., 2018). While the role of shootin1a phosphorylation is well understood, the molecular mechanism of shootin1a dephosphorylation is uncharacterized and its role in axon guidance remains unclear.

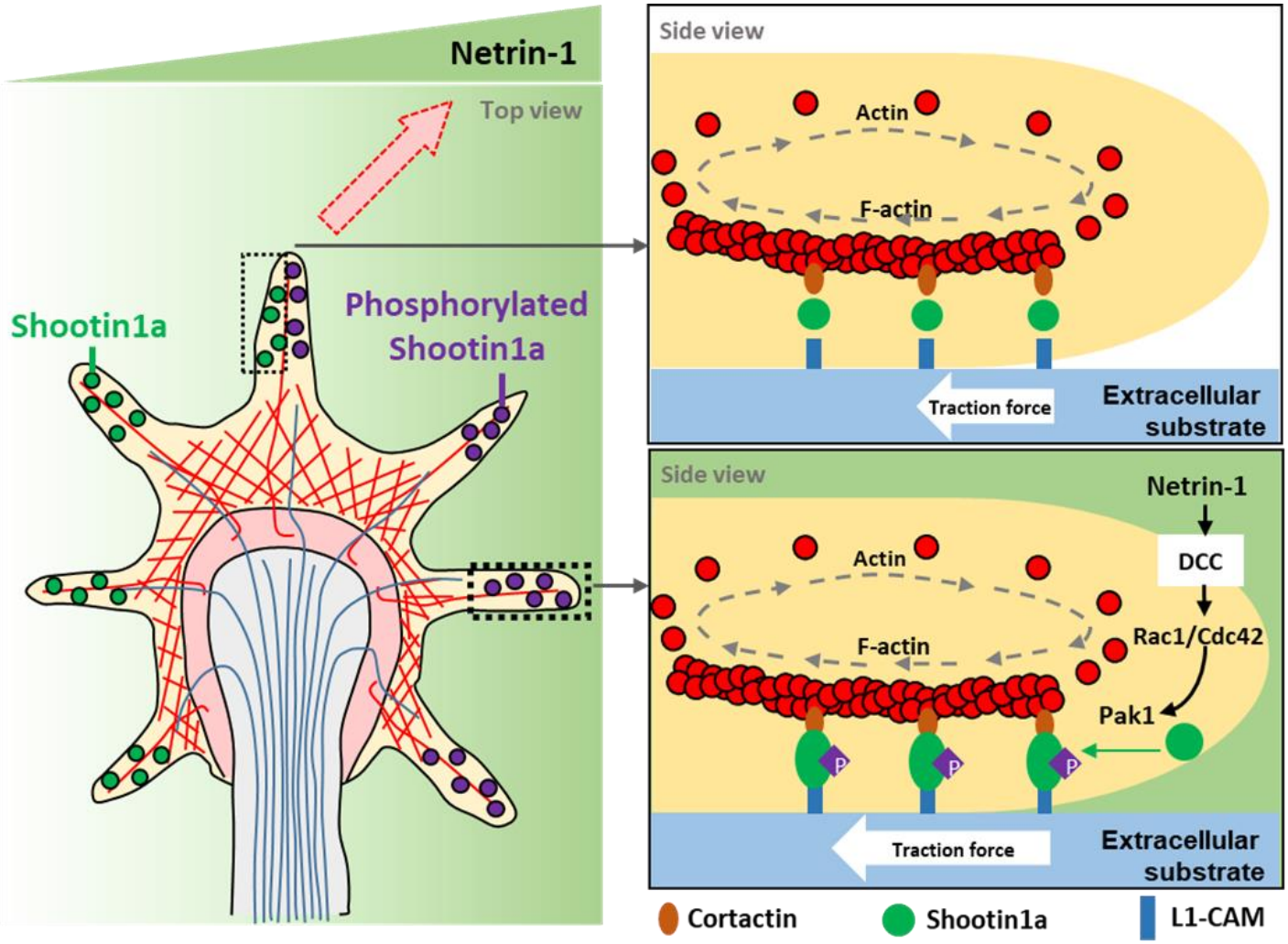

Figure 1 A model for gradient–reading processes of netrin-1–induced axon guidance

A small difference in netrin-1 concentration can induce highly polarized phosphorylation of shootin1a within growth cones. This process is transduced through a signaling pathway including DCC, Rac1/CDC42 and Pak1. The polarized phosphorylation of shootin1a within a growth cone locally promotes shootin1a–L1-CAM and shootin1a–cortactin interactions. These interactions in turn enhance directional traction force toward the netrin-1 source, thereby leading to a decision of the turning direction.

Protein phosphorylation is one of the most common and essential post-translation modifications (Li et al., 2013; Sacco et al., 2012). More than one-third of the protein phosphorylation events occurs on serine (Ser; S), threonine (Thr; T), and tyrosine residues (Tyr; Y). In human, approximately 568 protein kinases and 156 protein phosphatases regulate phosphorylation events and, play roles in the control of biological processes (Ardito et al., 2017). Protein phosphatases can be classified into three families defined by their catalytic domain sequence similarity; phosphoprotein phosphatase (PPP) family, metal-dependent protein phosphatase (PPM) family and protein-tyrosine phosphatase (PTP) family (Sacco et al., 2012) (Figure 2). The PPP family includes PP1, PP2A, PP2B/calcineurin, PP4, PP5, PP6 and PP7 responsible for several dephosphorylation events (Li et al., 2013) whereas PP2C is one of the most important member of the PPM family (Moorhead et al., 2009). PPP and PMP families are responsible for the majority of serine and threonine dephosphorylation reactions, and they also dephosphorylate tyrosine residue (Das et al., 1996; Shi, 2009).

The majority of neuronal serine or threonine dephosphorylation is mediated by the protein phosphatases type 1 (PP1), 2 (PP2A) and 3 (PP2B or calcineurin) (Figure 2). These phosphatases, together with protein kinases, not only contribute to the control of synaptic plasticity and memory, but also play roles in axon outgrowth (Monroe and Heathcote, 2013) and guidance for the neuronal network formation (Sutherland et al., 2014). It is clear that Pak1, upon activation by netrin-1, phosphorylates shootin1a, however, the phosphatases that responsible for shootin1a dephosphorylation are unidentified. In addition, the involvement of shootin1a dephosphorylation in axon guidance remains unclear. In this study, using pharmacological and biochemical evidence, I demonstrate that shootin1a is dephosphorylated by PP1 *in vitro* and *in vivo*. In addition, overexpression of PP1 disturbs netrin-1–induced asymmetric phosphorylated shootin1a localization within the growth cones, resulting in unresponsive axon turning under the netrin1 gradients.

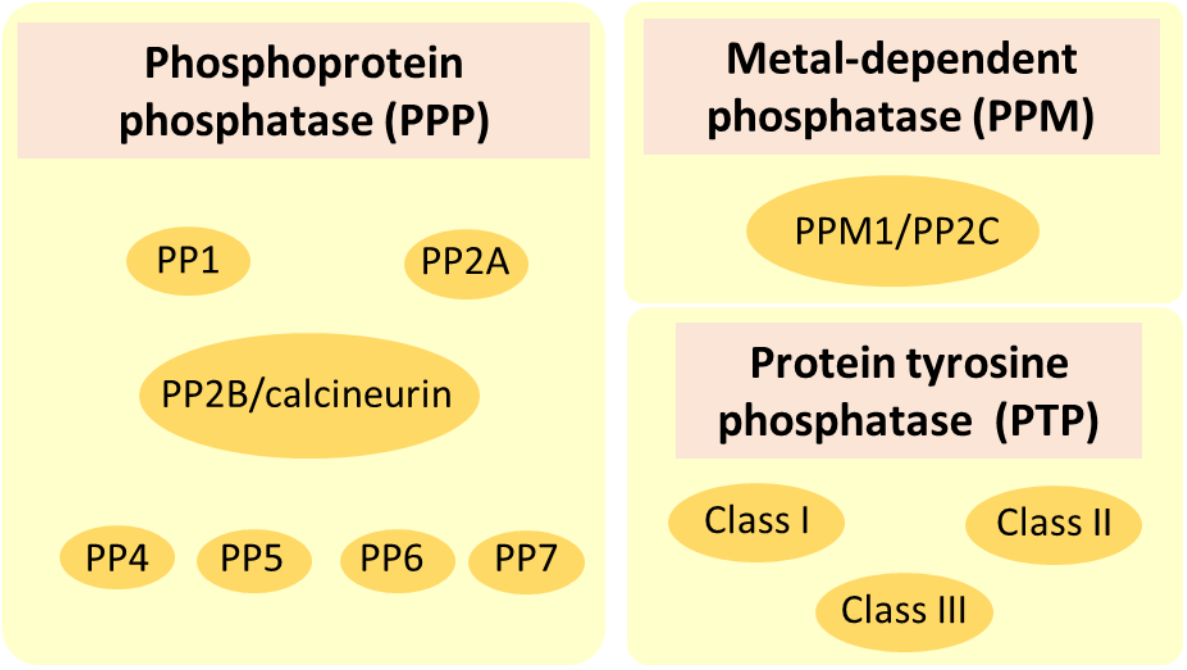

Figure 2 Protein phosphatase superfamily

The phosphoprotein phosphatase (PPP) and metal-dependent phosphatase (PPM) families encode protein serine/threonine phosphatases, whereas the protein tyrosine phosphatase (PTP) family includes both tyrosine-specific and dual-specificity phosphatases. The major serine/threonine protein phosphatases in the brain are PP1, PP2A and PP2B.

Materials and Methods

Culture of neurons

Cortical and hippocampal neurons were prepared from E16.5 mice and were cultured on glass coverslips coated with polylysine and polylysine with L1-CAM-Fc, respectively (Baba et al., 2018; Kubo et al., 2015; Shimada et al., 2008; Toriyama et al., 2013). Impregnated female mouse (purchased from SLC Japan or CLEA Japan) was anesthetized through inhalation of vaporized isoflurane. Whole embryonic brains were carefully removed and placed in 0.4% glucose in PBS solution. The hemispheres were then separated followed by removing meninges layer. Cortex and hippocampus were carefully dissected and incubated in A+ solution (0.5 mg/ml papain, 1 mg/ml BSA, 6 μg/ml DNase I, 0.01 M glucose, PBS) at 37°C water bath for 20 minutes. Solution A+ was discarded and replaced with A- solution (1 mg/ml BSA, 6 μg/ml DNase I, 0.01 M glucose, PBS). Cortex and hippocampus were dissociated by gently pipetting and incubated at 37°C water bath for 15 minutes. Genetic materials were removed from the cell suspension using a glass Pasteur pipette. Neurons were then collected by centrifugation (4°C, 2500 RPM, 3 minutes) and resuspended in PBS solution. Cell number was counted using hemocytometer with tryphan blue staining. Neurons were resuspended in 10% FBS in Neurobasal medium (Thermo Fisher Scientific). For the immunoblot experiment, cortical neurons were cultured on the petri dish (Matsunami) coated 100 μg/ml poly-D-lysine. For the immunostaining and live-cell imaging experiment, hippocampal neurons were cultured on the glass bottom dishes (Matsunami) coated poly-D-lysine and L1-CAM-Fc. The cultured neurons were incubated at 37°C, 5% CO_2 for 3 hours. Neurobasal Medium containing B-27 supplement (Thermo Fisher Scientific) and GlutaMAX. Neurons were then cultured until day *in vitro* (DIV) 1.5 - DIV3.

Transfection

Neurons were transfected with vectors using Nucleofector (Lonza) before plating. Neurons (1.0 x 10^6 cells) were suspended in 100 μL of Nucleofector™ solution with 1 - 2 μg of interested–plasmids. The suspension was transferred into an

electroporation cuvette. Recombinant plasmids were introduced into the mouse neurons, using an electroporator (Amaxa Biosystems). Transfected neurons were immediately transferred to Neurobasal Medium supplemented with 10% fetal bovine serum and 0.01% penicillin streptomycin. HEK293T (ATCC) and COS7 cells were cultured in Dulbecco's modified Eagle's medium (Sigma-Aldrich) supplemented with 10% fetal bovine serum (Japan Bio Serum) and transfected with plasmid DNA by Polyethylenimine MAX (PEI MAX, Polysciences).

DNA constructs

Preparation of the vectors to express FLAG-shootin1a has been described previously (Toriyama et al., 2006). PP1 catalytic subunit alpha (PPP1CA) was amplified from mouse brain cDNA using following primers: Forward 5'-ATGTCCGACAGCGAGAAGCT-3' and Reverse 5'-CTATTTCTTGGCTTTGGCGGAA TTGC-3'. PCR product was ligated to pCMV-myc and pCAGGS-EGFP expression plasmid with the digestion of BamHI/SacI and EcoRI/XhoI, respectively. pCAGGS-EGFP was used for protein overexpression under the β-actin promoter as described (Toriyama et al., 2006). Expression level of recombinant PP1 was determined in COS7 cells.

Immunoprecipitation and immunoblot

For determining phosphorylated shootin1a in phosphatases inhibition, DIV3 neurons (1 x 10^6 cells) were incubated for 1 hour with following phosphatases inhibitors: 200 nM calyculin A (PP1/PP2A inhibitor), 100 nM okadaic acid (PP1/PP2A inhibitor), 10 μM endothall (PP2A inhibitor), 10 μM deltametrin (PP2B inhibitor), and 10 μM sanguinarine chloride (PP2C inhibitor). For *in vivo* dephosphorylation assay of shootin1a, COS7 cells were transfected with pCMV-FLAG-shootin1a with or without pCMV-myc-PP1 using Polyethylenimine MAX (PEI MAX, Polysciences). Transfected COS7 cell lysates were then collected at 48 hours post-transfection.

The cell lysates were prepared using RIPA lysis buffer (25 mM Tris-HCl pH 8.0, 75 mM NaCl, 0.5 mM EDTA, 0.5% Triton X-100, 0.05% SDS, 0.05% deoxycholic

acid, 1 1mM DTT, 1 mM PMSF, 0.01 mM leupeptin, 5 mM NaF, 1xPhosStop). Immunoblot of phosphorylated shootin1a were then performed using 8% SDS-polyacrylamide gel and PVDF membrane. Phosphorylated shootin1a and total shootin1a were detected using the following antibodies: rabbit anti-pSer249-shootin1 (1:5000, PMID: 23453953), rabbit anti-pSer101-shootin1 (1:1000, PMID: 23453953), rabbit anti-shootin1a (1:10000, PMID: 30082022) (Baba et al., 2018; Toriyama et al., 2013), or mouse anti-PP1 (1:1000, Santa Cruz BioTechnology, Cat# sc-7482, Lot# E1619). The following secondary antibodies, HRP-conjugated donkey anti-rabbit IgG (1:2000, GE Healthcare, Cat# NA934) and HRP-conjugated goat anti-mouse IgG (1:2000, Bio-Rad, Cat# 1706516), were used in immunoblotting. Immunodetection was performed by using the enhance chemiluminescence system (ECL, Amersham, Bioscience). Chemiluminescent signals were projected on X-ray film and digitalized, and the signals were quantified using ImageJ.

For immunoprecipitation, HEK293T cells were transfected with pCMV-FLAG-shootin1a with or without pCMV-myc-PP1 using Polyethylenimine MAX (PEI MAX, Polysciences). Cell lysates were prepared using NP40 lysis buffer (0.5% NP-40, 20 mM HEPES-Na pH 7.5, 3 mM $MgCl_2$, 100 mM NaCl, 1 mM EGTA, 1 mM DTT, 1 mM PMSF, 0.01 mM leupeptin, 5 mM NaF, 1xPhosStop). For FLAG-shootin1a immunoprecipitation, the supernatants of cell lysates were incubated with 30 μl (bed volume) of anti-FLAG M2 gel (Sigma) for 4 hours at 4°C. For myc-PP1 immunoprecipitation, the supernatants of cell lysates were incubated with anti-myc mouse (2 μg; Medical & Biological Laboratories) for 2 hours at 4°C and followed by Protein-G-sepharose 4 Fast Flow (GE Healthcare) for 2 hours at 4°C. The immunoprecipitates were washed four times with wash buffer (0.1% Tween 20, 20 mM HEPES-Na pH 7.5, 3 mM $MgCl_2$, 100 mM NaCl, 1 mM EGTA, 1 mM DTT). To elute immunocomplexes, the gels were incubated with FLAG peptide (400 μg/ml) or myc peptide (1 mg/ml) for 1 hours at 4°C. The immunocomplexes were analyzed by immunoblot using anti-FLAG or anti-myc antibodies (Medical & Biological Laboratories).

Immunocytochemistry and microscopy

Cultured neurons were fixed with 3.7% formaldehyde dissolved in Krebs buffer (118 mM NaCl, 5.7 mM KCl, 1.2 mM KH_2PO_4, 1.2 mM $MgSO_4$, 4.2 mM $NaHCO_3$, 2 mM $CaCl_2$, 10 mM Glucose, 400 mM Sucrose, 10 mM HEPES-Na pH7.2) for 10 min at room temperature, followed by treatment with 0.05% triton X-100 in PBS for 15 min on ice and blocked 10 % fetal bovine serum in PBS for 1 hour at room temperature. They were then incubated using the following primary antibodies diluted with blocking serum: rabbit anti-shootin1a (1:2000, PMID: 30082022), rabbit anti-pSer249-shootin1 (1:2000, PMID: 23453953), or mouse anti-PP1 (1:500, Santa Cruz BioTechnology) overnight at 4°C. Neurons were washed in PBS and incubated with secondary antibodies conjugated with Alexa Fluor 488 (1:1000, Invitrogen) and Alexa Fluor 594 (1:1000, Invitrogen) for 1 hour at room temperature. For CMAC staining, cells were incubated with 2.5 mM CMAC for 1 hour before generation of netrin-1 gradients. Immunostained cells were mounted with 50% (v/v) glycerol (Nacalai Tesque) in PBS. Fluorescence images were acquired using either a fluorescence microscope (Axioplan2; Carl Zeiss Inc.) equipped with a plan-Apochromat 100 × 1.40 Oil objective (Carl Zeiss, Inc.), a charge-coupled device camera (CCD, AxioCam MRm, Carl Zeiss) and imaging software (Axiovision3, Carl Zeiss). Live-cell images of cultured hippocampal neurons were acquired at 37°C using a fluorescence microscope (IX81; Olympus) equipped with and EM-CDD camera (Ixon3; Andor), a CMOS camera (ORCA Flash4.0LT; Hamamatsu), an UplanApo 20 x 0.7 NA (Olympus), and imaging software (MetaMorph, molecular devices). Axon outgrowth, trajectories, and turning were measured using ImageJ (Fiji version).

Protein preparation and *in vitro* phosphatase assay

Phosphorylated shootin1a was expressed in HEK293T cells with FLAG tag. To increase phosphorylated shootin1a in HEK293T cells, transfected cells was treated with calyculin A (final concentration 200 nM) for 1 hour. Phosphorylated shootin1a was then purified using anti-FLAG M2 gels as described above. Recombinant PP1 alpha (NBP1-72418, Lot 18120801), PP2A alpha (14-111-D, Lot 2917662, 3183636),

PPM1A (ab128560) were purchased from Novus Biologicals, Millipore, and Abcam, respectively. Phosphatase reactions were carried out in PP1 reaction buffer (10 mM Tris-HCl pH 8.0, 50 mM NaCl, 2 mM DTT, 1 mM $MnCl_2$), PP2A reaction buffer (50 mM Tris-HCl pH 8.0, 150 mM NaCl, 1 mM DTT, 1 mM $MnCl_2$), PP2C reaction buffer (50 mM Tris-HCl pH 8.0, 0.1 mg/ml BSA, 1 mM DTT, 30 μM EDTA, 40 mM $MgCl_2$) containing 3.3, 8.3, 16.7 ng/μl PP1, PP2A, or PP2C and 0.015 μg phosphorylated shooin1a. The reactions were incubated at 30°C for 3 hours. Immunoblot of phosphorylated shootin1a was then performed.

Axon guidance assay

A microfluidic device that generates netrin-1 gradients in culture medium was produced according to a previous report (Baba et al., 2018; Bhattacharjee et al., 2010). Briefly, microfluidic device was fabricated with polydimethylsiloxane (PDMS; Silpot 184, Dow Corning Toray) and attached to a glass coverslip. The device consists of a close cell culture area and two microchannels along sides of the culture area. PDMS sheet was fabricated from the mold, which had been coated with silicone oil (Barrier coat No. 6, ShinEtsu). A PDMS sheet was then attached to a glass coverslip using plasma bonding (Sakigake). The glass coverslip was coated with polylysine and L1-CAM-Fc. Hippocampal neurons were transfected with pCAGGS-EGFP (control) or pCAGGS-EGFP-PP1. Transfected neurons at DIV1.5-2 were used for time-lapse imaging. To generate netrin-1 gradients in the cell culture area, culture medium with or without 300 ng/ml netrin-1 (R&D systems, Cat# 1109-N1-025, Lot# IPE2020041) were applied to the microchannels on either side of the cell culture area for 420 minutes. Analysis of turning angle under netrin-1 gradients. X and Y axis are set from the growth cone at first time-point. X axis was drawn along the axon shaft. Turning angles (θ) was measured angles between the first and last time-points of the observations.

Results

Inhibitors of PP1 increase phosphorylated shootin1a in hippocampal neurons

Previous studies have reported that netrin-1–induced shootin1a phosphorylation at Ser101 and Ser249 through p21-activated kinase 1 (Pak1) (Baba et al., 2018; Kubo et al., 2015; Toriyama et al., 2013). Reversible protein phosphorylation is regulated through a balance between protein kinases and phosphatases. To identify which phosphatases are involved in shootin1a dephosphorylation, five inhibitors of serine/threonine phosphatases were applied to DIV3 cultured hippocampal neurons. The following protein phosphatase inhibitors were used: 200 nM calyculin A (PP1/PP2A inhibitor), 100 nM okadaic acid (PP1/PP2A inhibitor), 10 μM endothall (PP2A inhibitor), 10 μM deltametrin (PP2B inhibitor), and 10 μM sanguinarine chloride (PP2C inhibitor). Application of calyculin A or okadaic acid showed that blocking PP1/PP2A activity increased endogenous phosphorylated shootin1a at Ser101 (pSer101) and Ser249 (pSer249) (Figure 3A and B, FigureS1 for full immunoblot scans). However, treatments of PP2A inhibitor endothall, PP2B inhibitor deltametrin, or PP2C inhibitor sanguinarine chloride did not affect phosphorylated shootin1a level (Figure 3A and B, FigureS1 for full immunoblot scans). These results suggest that PP1 may be a candidate phosphatase in shootin1a dephosphorylation.

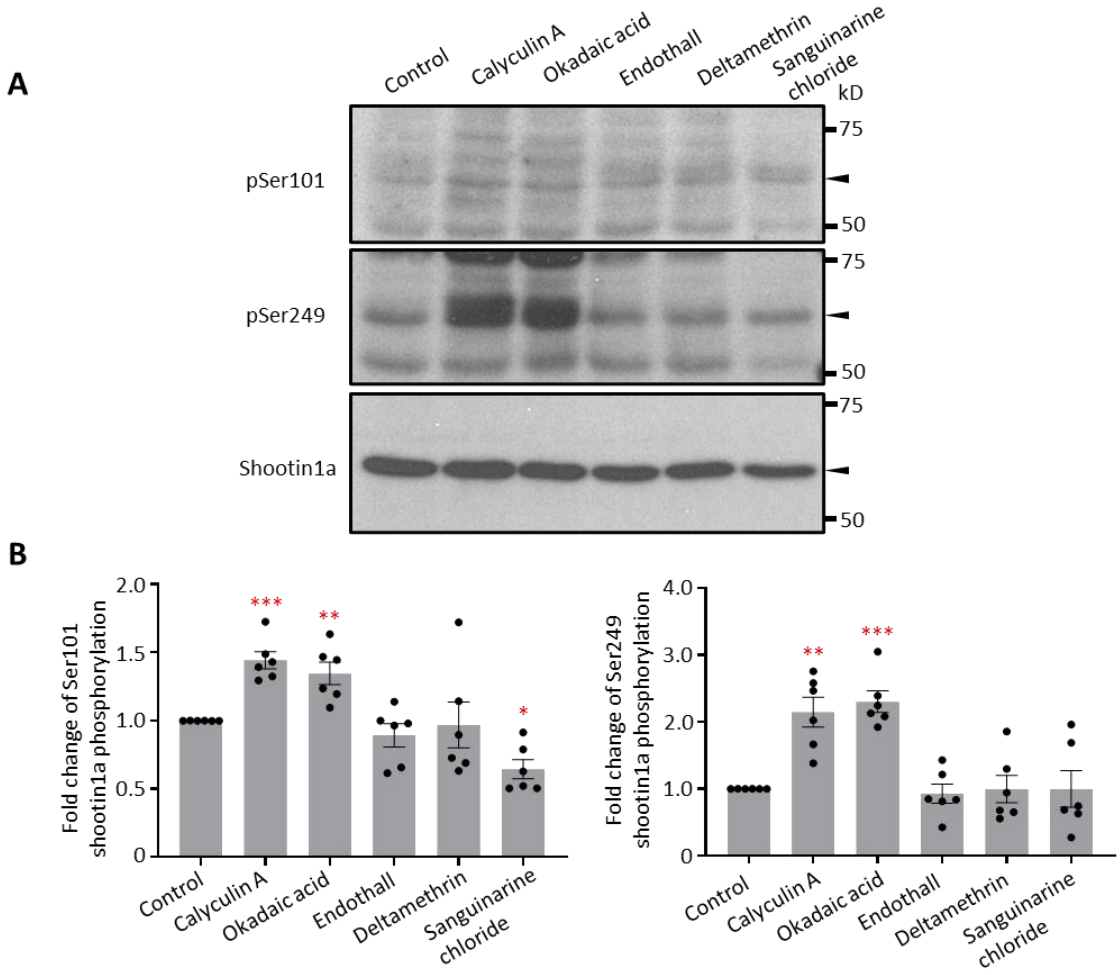

Figure 3 Inhibitors of PP1 increase phosphorylated shootin1a in hippocampal neurons

A. Cultured hippocampal neurons (DIV3) were treated with various phosphatase inhibitors: DMSO as a control, 200 nM calyculinA for PP1/PP2A, 100 nM okadaic acid for PP1/PP2A, 10 μM endothall for PP2A, 10 μM deltamethrin for PP2B, 10 μM sanguinarine chloride for PP2C. Protein lysates were prepared after 1 hour treatment and analyzed by western blotting with antibodies against pSer101, pSer249 and shootin1a. Arrowheads indicated shootin1a. The full-length images for western blots in Fig.3A were presented in supplementary figure 1.

B. Quantitative analysis of phosphorylated shootin1a at Ser101 and Ser249 is represented as the fold change relative to DMSO–treated neurons (n = 6). Data represent means ± SEM; ***<0.001, **p<0.01; *p<0.05 (unpaired Student's t-test)

PP1 dephosphorylates shootin1a *in vitro* and *in vivo*

To determine whether PP1 directly dephosphorylates shootin1a, an *in vitro* phosphatase assay was performed using purified phosphorylated shootin1a and PP1, PP2A, or PP2C. Shootin1a with N-terminal FLAG epitope tag (FLAG-shootin1a) was overexpressed in HEK293 cells. FLAG-shootin1a amino acid sequence was shown in FigureS4A. To increase shootin1a phosphorylation level, shootin1a–overexpressed HEK293T cells was then treated with 200 nM calyculin A before purification. Purity of phosphorylated shootin1a was shown in FigureS2C. Phosphorylated shootin1a was then incubated with PP1, PP2A, or PP2C catalytic subunit. As shown in Figure 4A and B, PP1 and PP2C significantly dephosphorylated shootin1a at both Ser101 and Ser249. Moreover, shootin1a at Ser101 was dephosphorylated at 8.3 and 16.7 ng/μl of PP2A. On the other hand, PP2A had no effect on phosphorylated shootin1a level at Ser249 (Figure 4A and B, FigureS2A for full immunoblot scans). These results suggest that PP1 and PP2C dephosphorylate shootin1a *in vitro*. I noted that PP2A might dephosphorylate at Ser101, rather than Ser249 of shootin1a. The majority serine/threonine dephosphorylation in neurons is mediated by PP1, PP2A, and PP2B (Hoffman et al., 2017). Therefore, PP1 was chosen for the further studies in shootin1a dephosphorylation.

The above effects of phosphatase inhibitors and *in vitro* dephosphorylation assay suggest shootin1a is dephosphorylated by PP1. To determine whether PP1 mediates shootin1a dephosphorylation *in vivo*, phosphorylated shootin1a level was determined in PP1–overexpressed COS7 cells. Catalytic subunit of PP1 alpha isoform (NP_114074.1) was amplified from mouse brain cDNA with size 1012 base pairs. PP1 with N-terminal myc epitope tag (myc-PP1) amino acid sequence was shown in FigureS4A. Moreover, myc-PP1 was successfully expressed in COS7 cells (FigureS4B). Western blot analysis showed that PP1 significantly reduced the level of phosphorylated shootin1a at both Ser101 and Ser249 (Figure 4C and D, FigureS2B for full immunoblot scans). I note that phosphorylated shootin1a at Ser101 has more sensitivity to PP1 than Ser249 in *in vivo* experiment. Together, these results indicate that PP1 dephosphorylates shootin1a *in vitro* and *in vivo*.

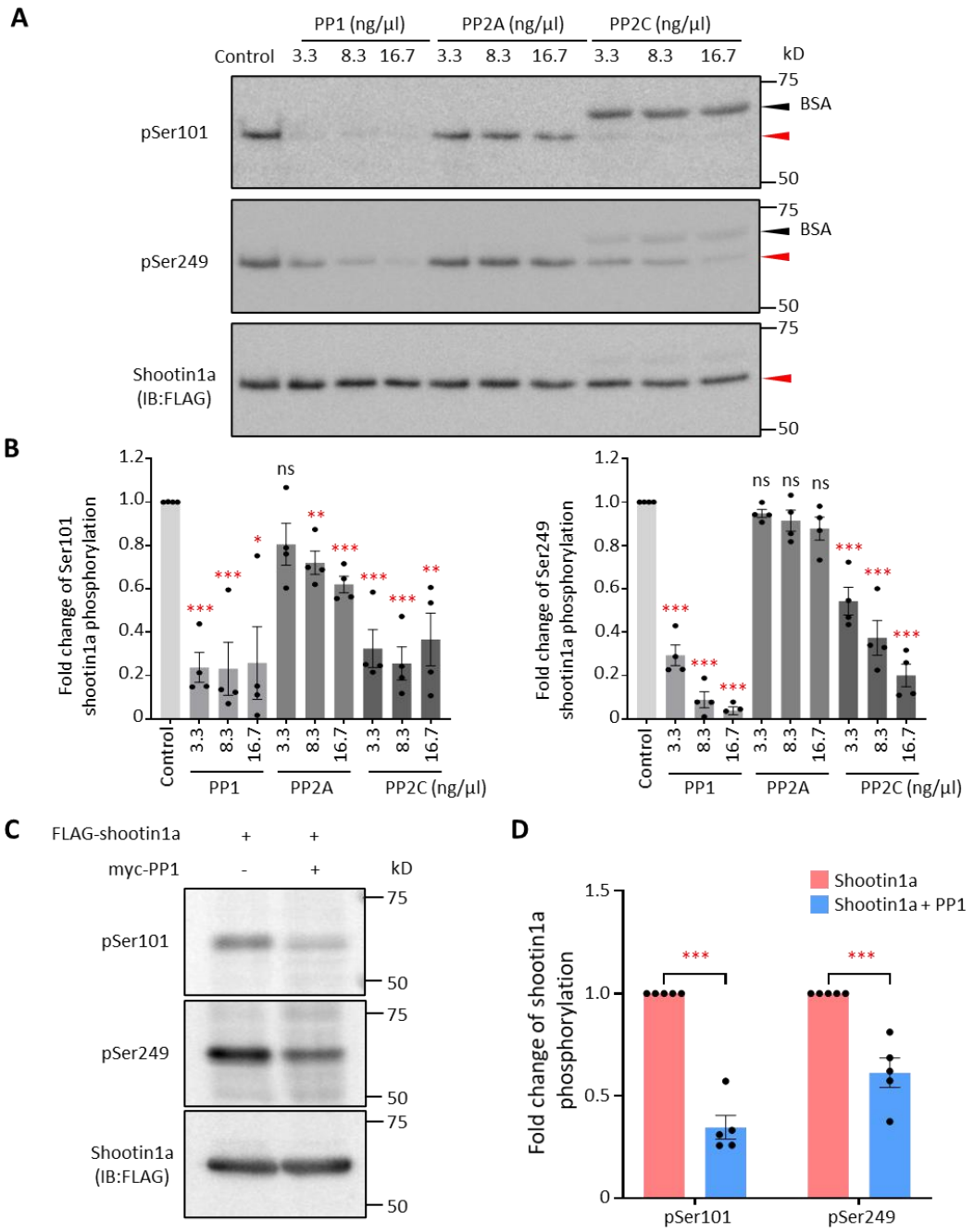

Figure 4 PP1 dephosphorylates shootin1a at Ser101 and Ser249 *in vitro* and *in vivo*

A. *In vitro* dephosphorylation assay was performed using purified phosphorylated shootin1a and PP1, PP2A or PP2C. FLAG-shootin1a was overexpressed in HEK293T cells followed by treatment of calyculin A for 1 hour. Phosphorylated FLAG-shootin1a was then purified by anti-FLAG agarose bead. After

dephosphorylation reaction with PP1, PP2A or PP2C (0, 3.3, 8.3, and 16.7 ng/μl), protein mixtures were subjected to SDS-PAGE followed by immunoblotted with antibodies against pSer101, pSer249 and FLAG tag. Red arrowhead indicated shootin1a. (n = 4)

B. Quantitative analysis of *in vitro* dephosphorylation assay of phosphorylated shootin1a at Ser101 and Ser249. The fold change of the phosphorylated shootin1a was calculated by normalizing to control. Data represent means ± SEM; ***p<0.001, **p<0.01, *p<0.05; ns, not significant, (unpaired Student's t-test).

C. Dephosphorylation of shootin1a by PP1 in COS7 cells. Cells were transfected with vectors to express FLAG-shootin1a and myc-PP1. Cell lysates were then subjected to SDS-PAGE followed by immunoblotted with antibodies against pSer101, pSer249 and FLAG tag. (n = 5)

D. Quantitative analysis of *in vivo* dephosphorylation assay of shootin1a by PP1 in COS7 cells. The fold change of the phosphorylated shootin1a was calculated by normalizing by lysates expressing only shootin1a. Data represent means ± SEM; ***p<0.001, (unpaired Student's t-test).

PP1 and shootin1a interaction is inconclusive

The PP1 activity toward shootin1a led me to further examine whether shootin1a interacts with PP1. To address this question, FLAG-shootin1a and myc-PP1 were co-expressed in HEK293T cells and their ability to bind each other was analyzed by immunoprecipitation assay. PP1 was detected in shootin1a immunoprecipitation by anti-FLAG agarose bead (Figure 5A, FigureS3A for full immunoblot scans). However, the reciprocal myc-PP1 coimmunoprecipitation did not show any signal of FLAG-shootin1a (Figure 5B, FigureS3B for full immunoblot scans). Therefore, the interaction of shootin1a and PP1 is inconclusive. Previous studies reported that phospho-mimic shootin1a (shootin1a-DD), in which Ser101 and Ser249 were replaced by aspartate, had stronger interaction with cortactin or L1-CAM than wild-type shootin1a (Baba et al., 2018; Kubo et al., 2015). Therefore,

PP1−induced shootin1a dephosphorylation may decrease interactions of shootin1a and partner proteins, including PP1.

Previous studies reported that phosphorylated shootin1a was highly colocalized with cortactin (Kubo et al., 2015) and L1-CAM (Baba et al., 2018) within axonal growth cones. To investigate whether PP1 localizes within the axonal growth cones, DIV2 hippocampal neurons were immunolabelled with a PP1 specific antibody. PP1 was localized in a "dot-like" pattern in the axonal growth cones. Interestingly, double fluorescence staining showed that shootin1a was partially colocalized with PP1 (Figure 5C). Together, these data suggest that shootin1a may be dephosphorylated by PP1 at axonal growth cones.

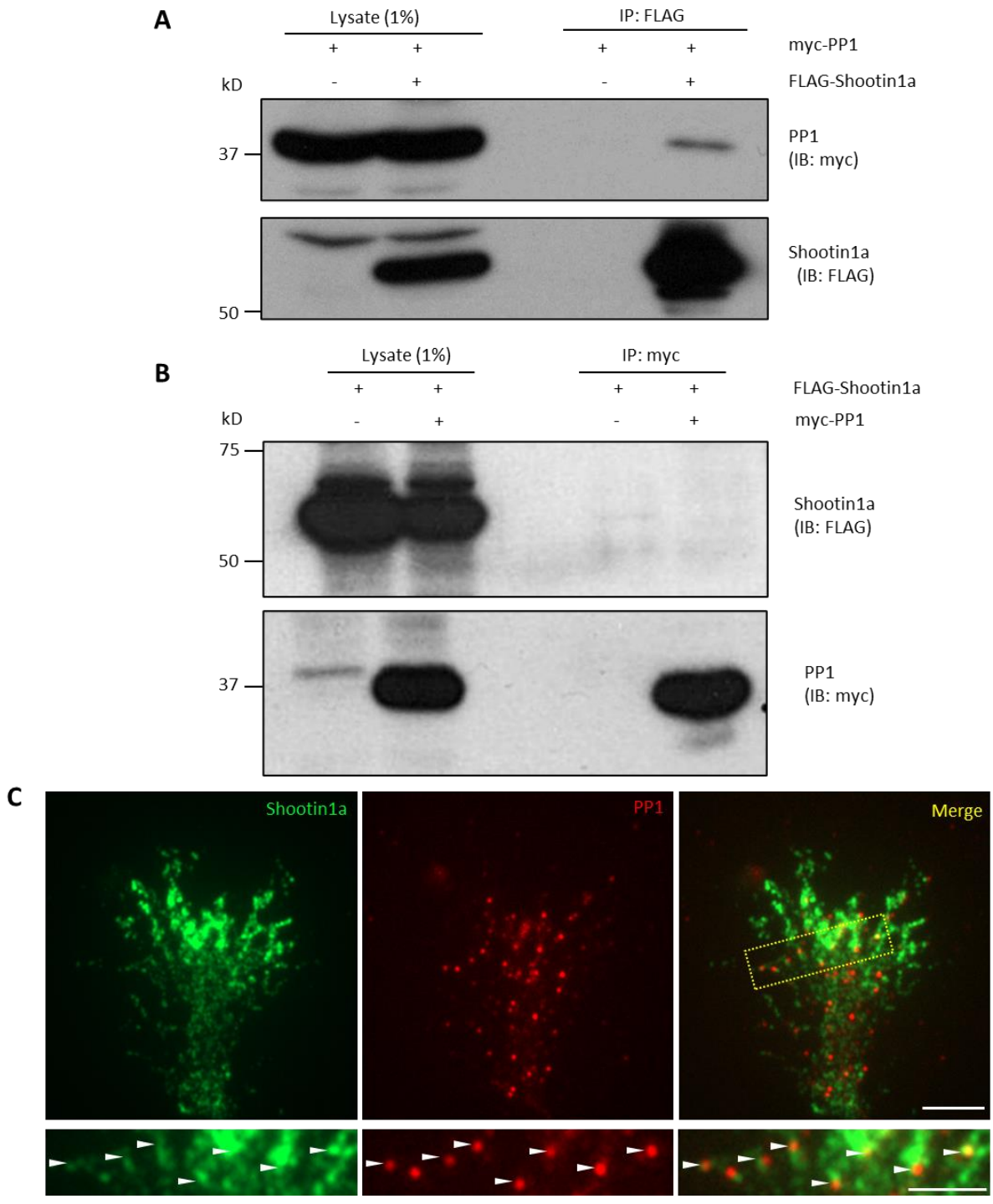

Figure 5 Shootin1a colocalized with PP1 at the axonal growth cones

A. Coimmunoprecipitation of FLAG-shootin1a and myc-PP1 in HEK293T cells. Cells were transfected with vectors to express FLAG-shootin1a and myc-PP1. Cell lysates were then incubated with anti-FLAG agarose bead. The cell lysates (1%)

and immunoprecipitates were immunoblotted with anti-myc or anti-FLAG antibody (n = 3).

B. Reciprocal coimmunoprecipitation of myc-PP1 and FLAG-shootin1a. HEK293T cells were transfected with vectors to express myc-PP1 and FLAG-shooin1a. Cell lysates were prepared and incubated with anti-myc antibody. The cell lysates (1%) and immunoprecipitates were immunoblotted with anti-myc or anti-FLAG antibody.

C. Fluorescence images of an axonal growth cone labeled with anti-shootin1a (green) and anti-PP1 (red) antibodies. An enlarged view of the growth cone in the rectangle is shown in the lower panel. Arrowheads indicate shootin1a colocalized with PP1. Bar: 5 μm (in the inset. 2 μm).

PP1 overexpression disturbs netrin-1–induced asymmetric phosphorylated-shootin1a localization within growth cones

A previous study reported that netrin-1 induces asymmetric localization of phosphorylated-shootin1a in axonal growth cones (Baba et al., 2018). I examined how does PP1 affect localization of netrin-1–induced shootin1a phosphorylation within growth cones. PP1–overexpressed plasmid with EGFP at the N-terminus was constructed under CAG promoter (Figure S4A). Recombinant EGFP-fused PP1 was successfully expressed in COS7 cells (Figure S4B). PP1–overexpressed neurons cultured in the device for 2 days were labeled with fluorescent volume marker 7-amino-4-chloromethylcoumarin (CMAC) and exposed to netrin-1 gradients for 30 minutes. The neurons were then fixed and immunolabeled with an antibody that recognizes shootin1a phosphorylation at Ser249. Specificity of phosphorylated shootin1a antibody at Ser249 was determined in wild-type and shootin1 knockout neurons. Phosphorylated shootin1a was detected in axonal growth cones of wild-type neurons, but disappeared in shootin1 knockout neurons (FigureS5A). Quantification of phosphorylated shootin1a immunoreactivity and CMAC staining revealed a highly polarized localization of the phosphorylated shootin1a within control growth cones (Figure 6A). The relative level of the phosphorylated shootin1a (phosphorylated

shootin1a immunoreactivity/CMAC staining) was higher 1.38 fold on the netrin-1 source side than on the control side (n = 44). Interestingly, overexpression of PP1 inhibited the asymmetric of phosphorylated shootin1a localization under netrin-1 gradient (n = 49) (Figure 6B). This result suggested that PP1 overexpression disturbs netrin-1–induced polarized shootin1a phosphorylation within growth cones.

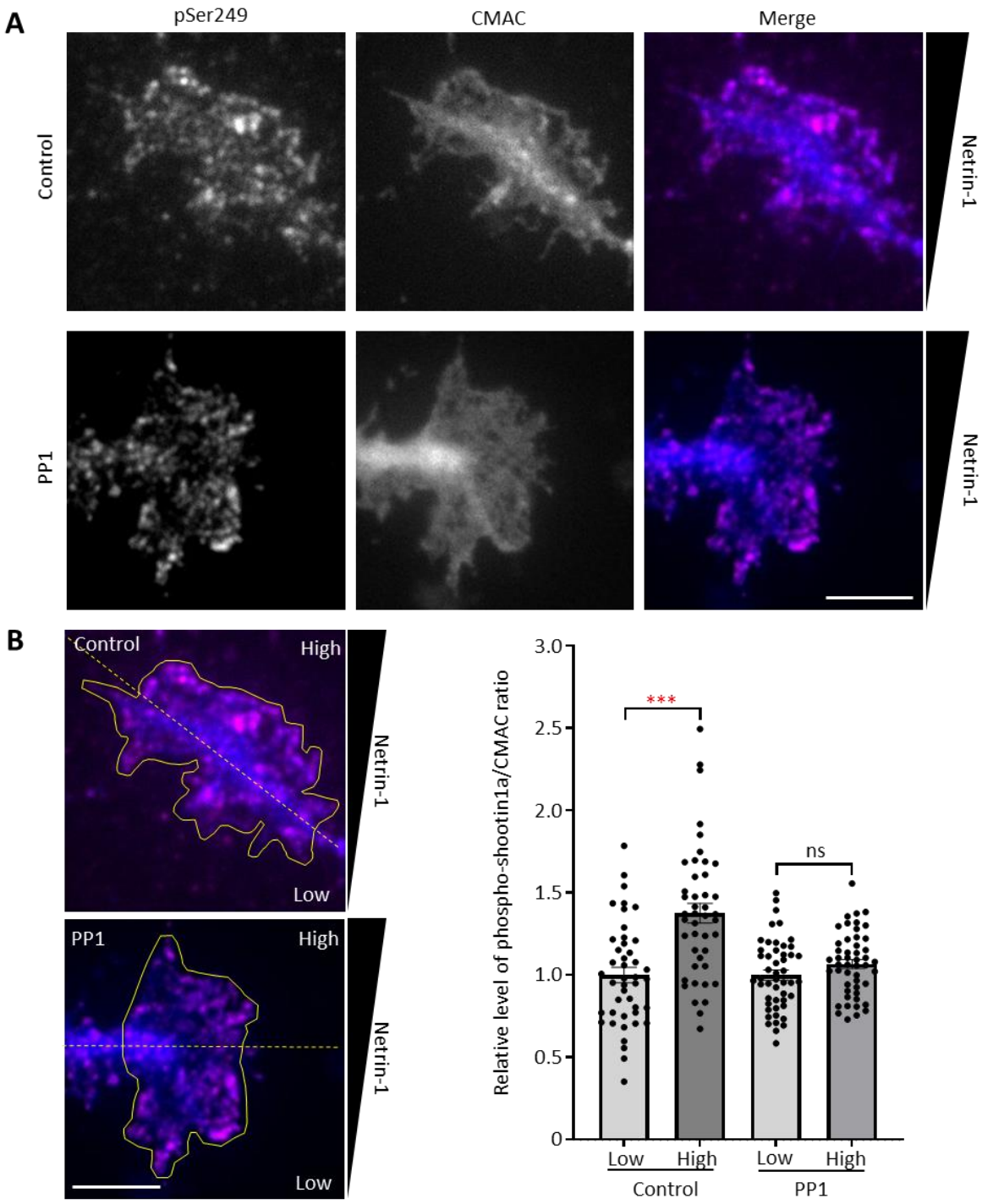

Figure 6 PP1 overexpression disturbs netrin-1–induced asymmetric phosphorylated-shootin1a localization within growth cones

A. Neurons were transfected with EGFP (control) or EGFP-PP1 (PP1) overexpression plasmid. Transfected neurons cultured in the device were labeled with CMAC (blue) and exposed to gradients of netrin-1 for 30 min. Netrin-1–

treated neurons were then fixed and immunolabeled with an antibody that recognizes shootin1a phosphorylation at Ser249 (magenta).

B. Quantification of relative phosphorylated shootin1a immunolabeling levels in PP1-overexpressing neurons. Yellow lines and dotted lines indicate the boundary and center line of the growth cone, respectively. Relative phosphorylated shootin1a immunolabeling levels (phosophorylated shootin1a immunoreactivity/ CMAC staining) quantification in the netrin-1 source side (high) and control side (low) of single growth cones. (n = 44, control; n = 49, PP1) Data represent means ± SEM; ***p<0.01, ns, not significant (unpaired Student's t-test). Bar: 5 μm

PP1 overexpression disturbs netrin-1–induced axon guidance

Shootin1a phosphorylation is required for axon outgrowth and guidance (Baba et al., 2018; Kubo et al., 2015). Moreover, disturbance of netrin-1–induced asymmetric phosphorylated shootin1a localization was observed in PP1–overexpressed neurons. Next, I examined whether the change of phosphorylated shootin1a localization by PP1 affects in axon outgrowth and turning. To address this question, axon guidance assay under netrin-1 gradient was then performed. Hippocampal neurons were transfected with EGFP (control) or EGFP-PP1 overexpression plasmid. Netrin-1 gradient was perpendicularly applied to the extending axons direction and its turning was recorded for 420 minutes. The below panels of Figure 7A represents the migration of individual axonal growth cones. The majority of axonal growth cones extended toward the netrin-1 source. The average netrin-1–induced axon outgrowth decreased in PP1–overexpressing neurons (Figure 7B). The average axon outgrowth velocity was 11.12 ± 1.70 μm/h (Figure 7C), and the net change in the angle of the growth cone toward the netrin-1 source was 47.12 ± 3.97° (n = 22) (Figure 7E). Dephosphorylation of shootin1a by PP1 overexpression not only reduced the axon outgrowth velocity (3.94 ± 0.32 μm/h) (Figure 7C) but also inhibited the growth cone turning toward the netrin-1 source (0.52 ± 8.93°, n = 20) (Figure 7E). These results suggest that PP1 at the cellular level is involved in netrin-1–induced axon guidance.

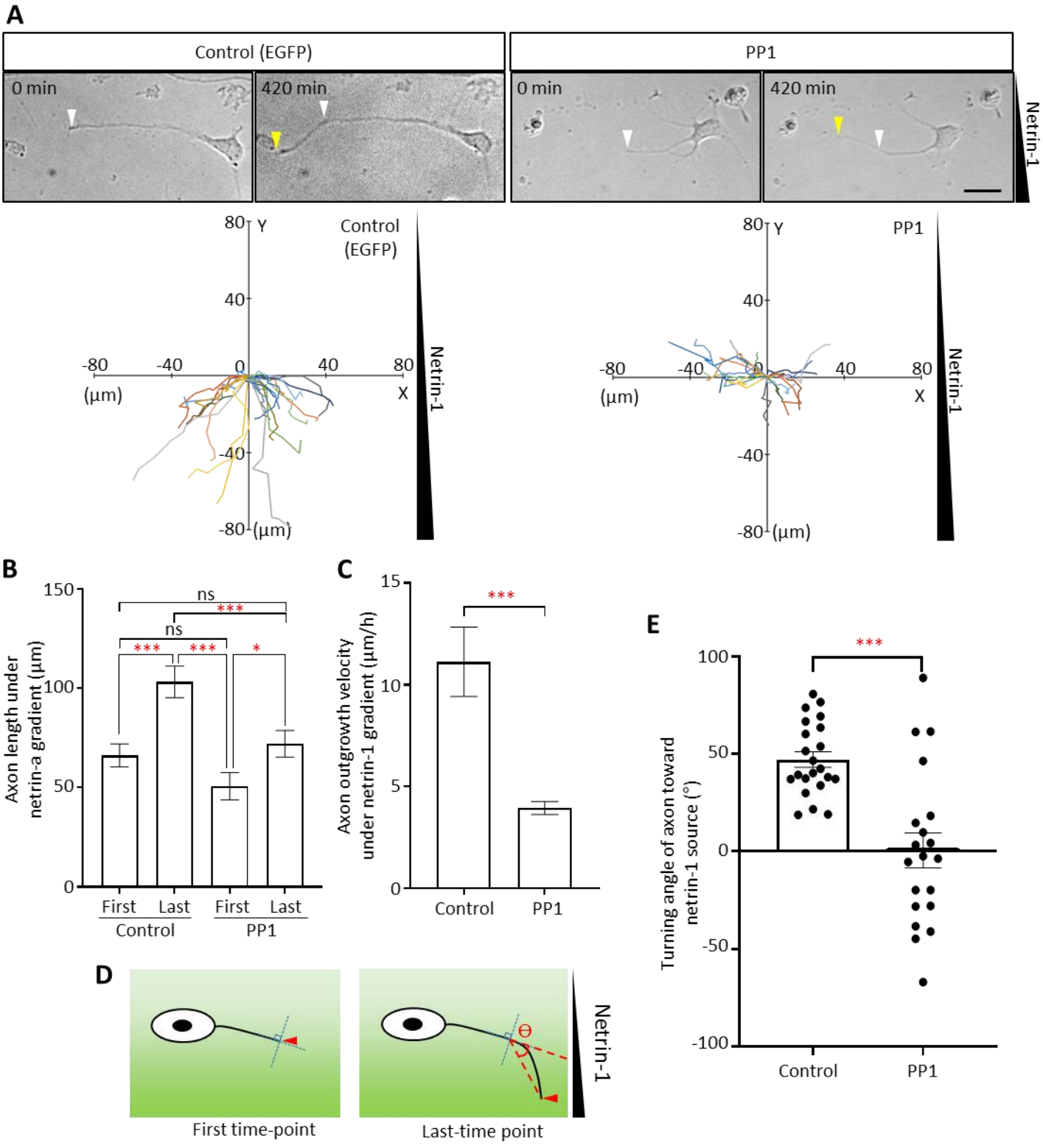

Figure 7 PP1 overexpression disturbs netrin-1–induced axon guidance

A. Time-lapse images of hippocampal neurons overexpressing EGFP (control) and EGFP-PP1 (PP1) under the gradients of netrin-1. White and yellow arrowheads indicate growth cones at the first and last time-points, respectively. The below panels depict trajectories of individual growth cone migrations. The initial growth cone positions are normalized at (x = 0 μm, y = 0 μm). Bars: 20 μm.

B. Axon length from first time-point (First; 0 minute) to last time-point (Last; 420 minutes) under netrin-1 gradients. Data represent means ± SEM; ***p<0.001, *p<0.05; ns, not significant (unpaired Student's t-test).

C. Axon outgrowth velocity was obtained from the analyses in A (n = 22, control; n = 20, PP1) Data represent means ± SEM; ***p<0.001 (unpaired Student's t-test)

D. Analysis of turning angle under netrin-1 gradients. X and Y axis were set from the growth cone at first time-point (red arrowhead). X axis was drawn along the axon shaft. Turning angles (θ) was obtained from analyses in A, by measuring angles between the first and the last time-points of the observations.

E. Turning angle of axon toward the netrin-1 source was measured from control or PP1–overexpressing neurons. The graph shows quantified data (n = 22, control; n = 20, PP1). Data represent means ± SEM. ***p < 0.01; (unpaired Student's t-test).

Discussion

Protein phosphorylation is a reversible process maintained by a balance between protein kinases and phosphatases that are crucial in neuronal network formation (Buchser et al., 2010; Carmody et al., 2004). Previous study reported that Pak1–induced shootin1a phosphorylation is critical for axon outgrowth (Kubo et al., 2015; Toriyama et al., 2013) and axon guidance (Baba et al., 2018). Here, I demonstrated that PP1 is responsible for shootin1a dephosphorylation both *in vitro* and *in vivo*. In addition, the cellular activity of PP1 has a role in netrin-1–induced asymmetric phosphorylated shootin1a localization and netrin-1–induced axon attraction.

The majority neuronal cell serine/threonine dephosphorylation is mediated by PP1, PP2A, and PP2B or calcineurin (Hoffman et al., 2017) (Figure 2). Therefore, the specific inhibitors of these phosphatases were selected as shootin1a dephosphorylation candidates. Calyculin A and okadaic acid, PP1/PP2A inhibitors, have been widely used in protein dephosphorylation studies. Analysis of okadaic acid–induced neuronal phosphoproteome previously reported that 245 phosphoproteins were significantly increased. Interestingly, shootin1 was found in the high protein phosphorylation state in response to okadaic acid treatment (Oliveira et al., 2017). Consistently, treatment of calyculin A or okadaic acid increased endogenous shootin1a phosphorylation level in neurons (Figure 3A and B). Thus, shootin1a dephosphorylation is inhibited through the repression of PP1/PP2A activity via okadaic acid.

Phosphatase inhibitors in several cell types have limitation in the interpretation of studies (Swingle et al., 2007), in particular in PP1 and PP2A which IC_{50} valued of such phosphatase inhibitors are almost identical (Gupta et al., 1997). Calyculin A and okadaic acid were firstly chosen to characterize a role of shootin1a dephosphorylation in axon guidance. Calyculin A is a strong inhibitor of PP1 and PP2A. A marked increase in phosphorylated shootin1a was detected in calyculin A–treated neurons (Figure 3A and B). However, the calyculin A treatment rapidly collapsed axonal growth cones (Figure S5B), consistent with earlier reports that

calyculin A induced growth cones collapse followed by axon retraction (Gungabissoon and Bamburg, 2003; Inutsuka et al., 2009; Kolpak et al., 2009). Calyculin A is retorted to generate strong contractile forces by actomyosin contraction, to induce rapid neurite retraction (Inutsuka et al., 2009). Okadaic acid at 100 nM, sufficient to inhibit PP1 and PP2A, not only increased phosphorylated shootin1a (Figure 3), but also induced the growth cones collapse (Figure S5B), which is consistent with prior studies (Das and Miller, 2012; Nakayama et al., 1999). Moreover, a low concentration of okadaic acid (5 nM) treatment specifically inhibits only PP2A, not PP1. Therefore, specific PP1 inhibitors, tautomycin or tautomycetin, are required for further determining the role of PP1 in shootin1a dephosphorylation involved in axon guidance.

Here, *in vitro* and *in vivo* dephosphorylation assay clearly confirmed that PP1 is a protein phosphatase responsible for shootin1a dephosphorylation (Figure 4). In neurons, PP1 plays roles in many processes including, synapse formation (Malchiodi-Albedi et al., 1997), neurotransmission (Colbran, 2004), neurite outgrowth (Oliver et al., 2002) and axon guidance (Wen et al., 2004). For vertebrates, approximately 200 PP1-interacting proteins (PIPs) have been studied. My study reported that interaction of PP1 and shootin1a is inconclusive. Phosphomimic shootin1a enhanced the interaction to partner proteins, cortactin or L1-CAM (Baba et al., 2018; Kubo et al., 2015). Therefore, dephosphorylated shootin1a by PP1 may reduce the binding affinity of shootin1a-PP1 interaction (Figure 5B). Profilin-1, actin-binding protein involved in the dynamic of the actin cytoskeleton, has been shown the less interaction to PP1 in the dephosphorylated form (Shao and Diamond, 2012). Second possibility is detected–PP1 in FLAG-shootin1a immunoprecipitation may be the result of shootin1 aggregation (Figure 5A). Shootin1a amino acid sequence contains the disordered region, particularly at the N-terminus, which might cause protein aggregation. Last, the epitope tagging position may interfere the protein folding or structure and disrupt protein-protein interaction. Therefore, the interaction of shootin1a and PP1 with C-terminal fusion tag will be further determined.

Dynamic subcellular localization of kinase and phosphatase activities leads us to understand the regulation of cellular functions through protein phosphorylation and dephosphorylation (Inagaki et al., 1994). Phosphorylated shootin1a accumulated at the axonal growth cones which highly colocalized with cortactin (Kubo et al., 2015) and L1-CAM (Baba et al., 2018). Previous study reported that Pak1, a key kinase for shootin1a phosphorylation, strongly enriched at the tips of filopodia (Robles et al., 2005). These data raise a possibility that shootin1a is phosphorylated at the tips of filopodia by Pak1. On the other hand, PP1 is distributed not only at filopodia tips but also in more proximal region of the growth cones and partially colocalized with shootin1a (Figure 5B). Therefore, shootin1a may be dephosphorylated by PP1 at the central region of the growth cone. Together, I consider that the reversible shootin1a phosphorylation is regulated by distinct subcellular localization of Pak1 and PP1 (Figure 8). Shootin1a moves retrogradely at the peripheral region of the growth cones (Toriyama et al., 2013). Therefore, the phosphorylation and dephosphorylation of shootin1a may be involved in recycling of shootin1a for axon extension (Figure 8).

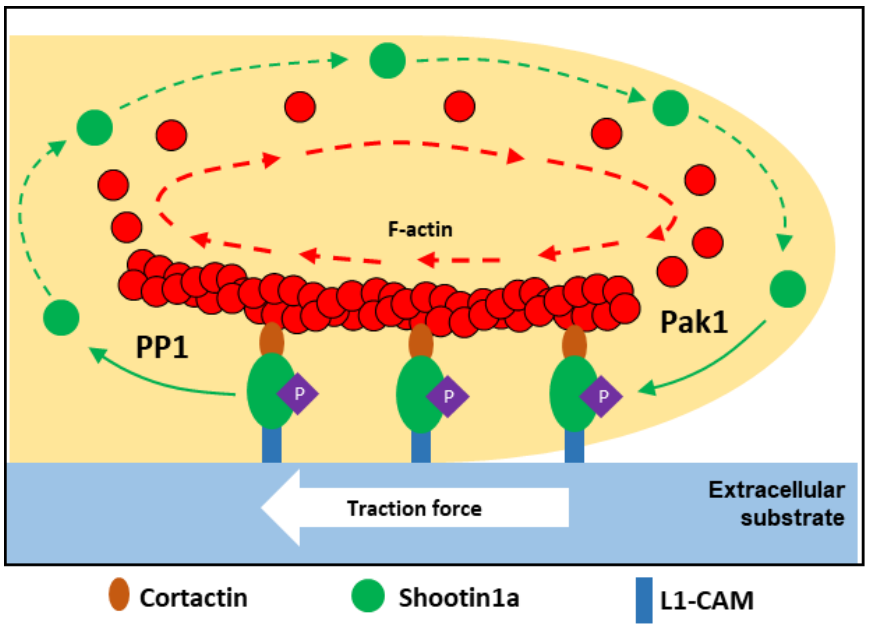

Figure 8 Distinct subcellular localizations of Pak1 and PP1 for reversible phosphorylation of shootin1a within axonal growth cones.

Shootin1a interacts with F-actin retrograde flow via cortactin and extracellular substrate via L1-CAM. Shootin1a is phosphorylated by Pak1 at the

leading edge of axonal growth cones, resulting in enhancement of traction force for growth cone migration. On the other hand, PP1 is a phosphatase that is responsible for shootin1a dephosphorylation at the central region of the growth cones.

The spatial and temporal regulation of protein localization within the growth cones is an important aspect of the mechanisms in axon guidance. Extracellular gradient of axon guidance cue elicits not only the polarized activation or repression of intracellular signaling pathways, but also the asymmetric distribution of proteins including cytoskeletal proteins and cell surface receptors in the growth cones (Bouzigues et al., 2007; Leung et al., 2006; Lin and Forscher, 1993; Yao et al., 2006). Moreover, post-translational modifications are essential for axon turning such as ubiquitination (Boyer et al., 2020; Menon et al., 2015) and phosphorylation (Baba et al., 2018).

Our laboratory previously reported that shootin1a phosphorylation within growth cones is required for netrin-1–induced axon turning. The small spatial differences in netrin-1 concentration on one side of the tip of an axon elicited highly polarized directional phosphorylation of shootin1a within growth cones (Baba et al., 2018). Local netrin-1 signal has been shown to promote polarized distribution of DCC orthologs UNC-40 in *C. elegans* (Killeen et al., 2002; Wang et al., 2014; Ziel et al., 2008). On the other hand, DCC on the surface of mouse cortical neurons did not show asymmetric localization under netrin-1 gradients (Taylor et al., 2015). My study suggests that PP1 disturbs the asymmetric phosphorylated shootin1a localization under netrin-1 gradients. Therefore, reversible shootin1a phosphorylation is one of the mechanisms which regulate the axon guidance.

Inhibition of actin retrograde flow and adhesion substrate engagement by shootin1 RNAi significantly decreased netrin-1–promoted axon outgrowth. Moreover, expression of RNAi-refractory WT and phosphomimic shootin1 rescued the reduction of axon length by shootin1 RNAi, but dephosphomimic shootin1 had no effect (Toriyama et al., 2013). Consistently, netrin-1–promoted axon outgrowth was

suppressed by PP1–induced shootin1a dephosphorylation in neurons, resulting in the reduction of axon outgrowth velocity (Figure 7).

Several phosphatases could affect the length of developing neurites during morphogenesis. Previous study reported that inhibition of PP1 activity reduced hippocampal neurite length and branching (Monroe and Heathcote, 2013). PP1 inhibition reduces growth by affecting adhesive pathways of hippocampal neurons including glycogen synthase kinase 3ß (GSK3ß) and focal adhesion kinase (FAK) (Bianchi et al., 2005). Moreover, blocking PP1 activity reduces growth cone motility by inhibiting non-muscle myosin II (Vereshchagina et al., 2004; Vicente-Manzanares et al., 2009). Overexpression of PP1 promotes nerve growth factor (NGF)–induced differentiation of PC12 to neuronal cells (Li et al., 2007). To date, there is no report on PP1 overexpression effect on axon outgrowth under netrin-1 gradients. My study suggested that netrin-1–induce axon outgrowth was suppressed in PP1–overexpressing neurons.

Previous work in *Xenopus* spinal neurons has shown that Ca^{2+}-calmodulin-dependent protein kinase II (CaMKII) and PP1 are involved in switching axon turning direction between attraction and repulsion (Wen et al., 2004). However, the downstream targets of PP1 in axon guidance is still elusive. Here, I showed the shootin1a dephosphorylation by PP1 disturbed netrin-1–induced axon turning (Figure 7A and E). My data demonstrated for the first time that dephosphorylation of shootin1a mediates in netrin-1–induced axon guidance.

Post-translational phosphorylation regulates the function of proteins through conformational changes. AlphaFold is a recently developed artificial intelligence system that predicts a protein structure based on its amino acid sequence (Jumper et al., 2021). Shootin1b structure, shootin1a extended isoform with 631 amino acid residues, was lately predicted from AlphaFold database (Figure 9). In human shootin1b, the three amino acids ASQ at the C-terminus of shootin1a are substituted by 178 amino acid residues. The predicted structure suggests that shootin1b may contain three α-helices at the N-terminus and disordered region at the C-terminus (Figure 9). Phosphorylation sites of shootin1b at Ser101 and Ser249 localized at the

first and second α-helices region, respectively. However, experimental approaches have been unsuccessful in determining the three-dimensional structure of shootin1a. Therefore, the molecular structure of shootin1a will be further studied. Furthermore, investigating of how the conformational changes of shootin1a phosphorylation mediated shootin1a–cortactin and shootin1a–L1-CAM interaction, will help to a better understanding of this mechanism.

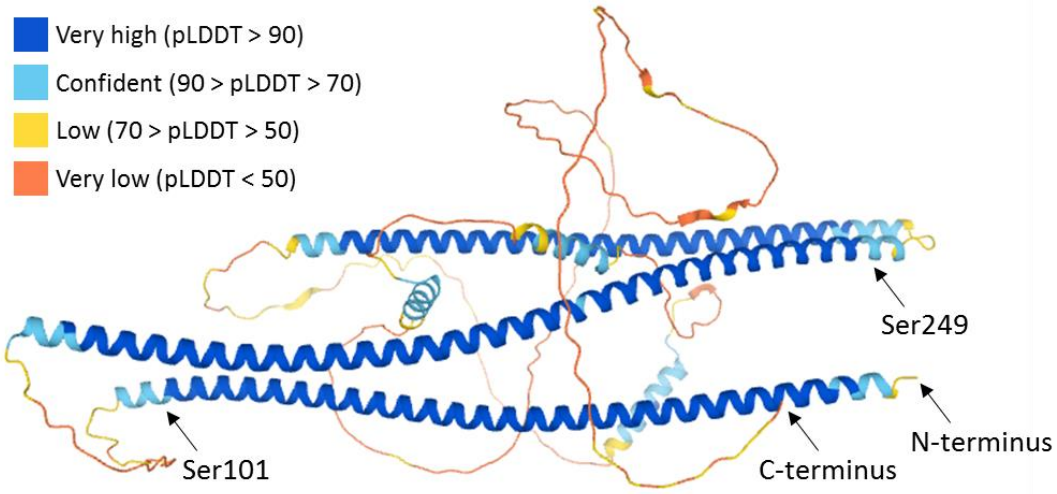

Figure 9 Shootin1b structure prediction from AlphaFold protein structure database.

Shootin1b structure was predicted using AlphaFold. N-terminal domain consists of three α-helices (blue). C-terminal domain contains disordered region (orange). The colors represent a confidence score (pLDDT) for each amino acid residue that ranges from 0 to 100.

PP1 classically consists of a complex of the catalytic subunit and one or more regulatory subunits (Cohen, 2002; Heroes et al., 2013; Hoffman et al., 2017; Inagaki et al., 1994). The nearly 200 vertebrate PP1–interacting proteins have already been identified and more than 70% of them have an annotated function (Heroes et al., 2013). At present, it is unknown which PP1–interacting proteins are responsible for shootin1a dephosphorylation. In addition, how shootin1a dephosphorylation is regulated by extracellular guidance molecules remains unclear. Detailed mechanisms for the regulation of PP1–mediated shootin1a dephosphorylation remain for future analyses.

Supplemental Figures

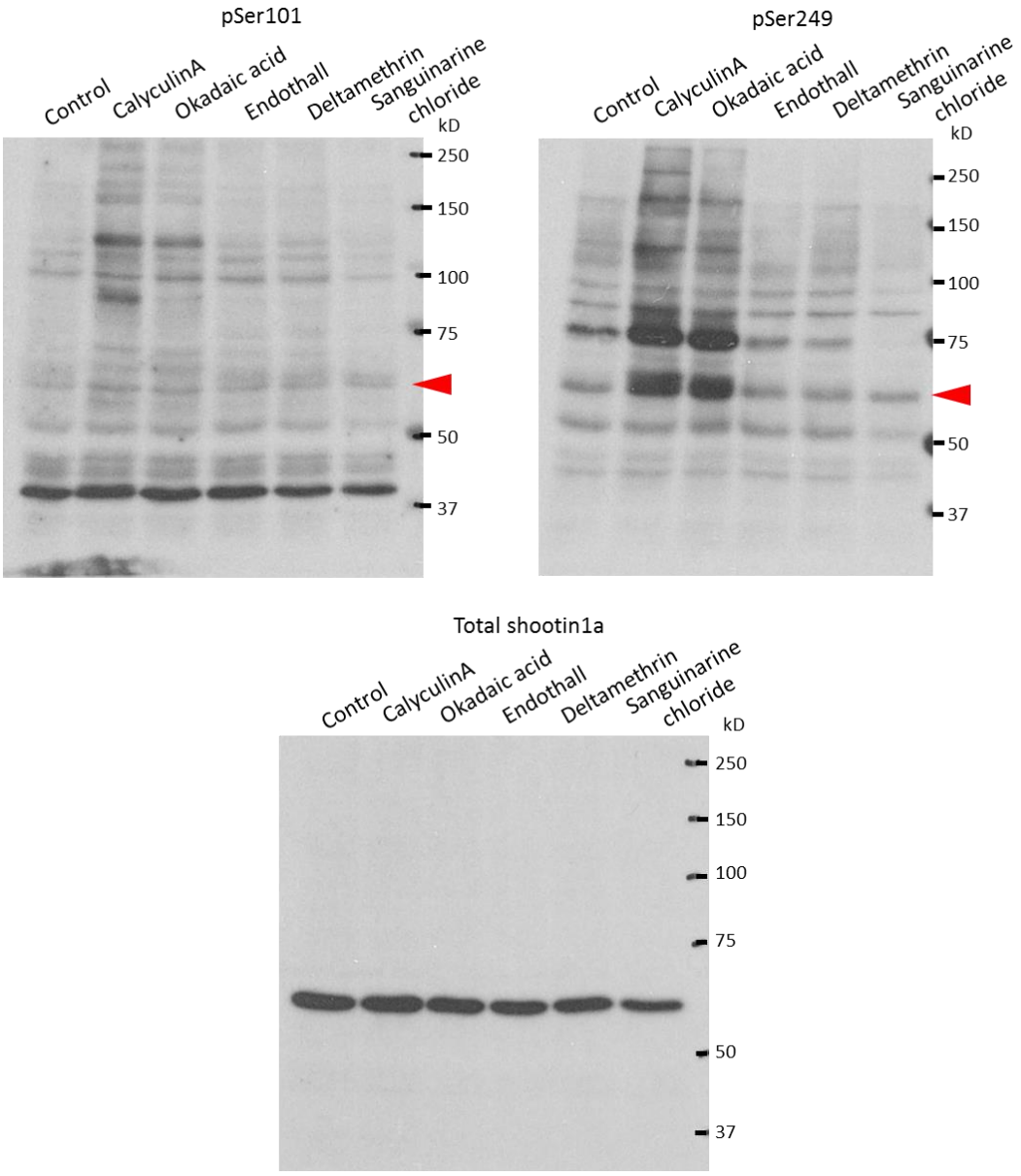

Figure S1 Inhibitors of PP1 increase phosphorylated shootin1a in hippocampal neurons

Cultured hippocampal neurons (DIV3) were treated with various phosphatase inhibitors: DMSO as a control, 200 nM calyculinA for PP1/PP2A, 100 nM okadaic acid for PP1/PP2A, 10 μM endothall for PP2A, 10 μM deltamethrin for PP2B, 10 μM sanguinarine chloride for PP2C. Protein lysates were prepared after 1 hour treatment and analyzed by western blotting with antibodies against pSer101, pSer249 and shootin1a. Red arrowheads indicated phosphorylated shootin1a.

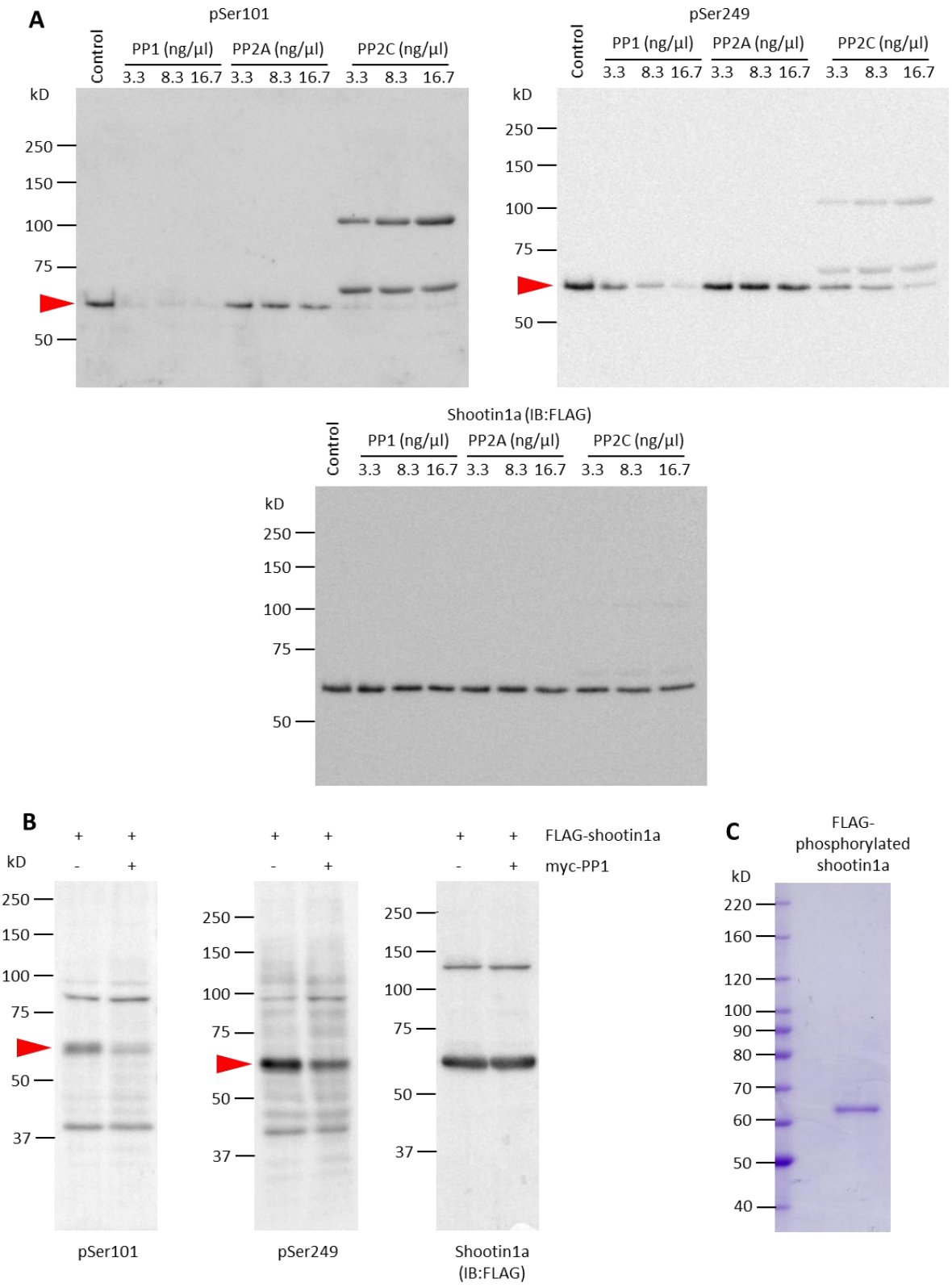

Figure S2 PP1 dephosphorylates shootin1a at Ser101 and Ser249 *in vitro* and *in vivo*

A. *In vitro* dephosphorylation assay was performed using purified phosphorylated shootin1a and PP1, PP2A or PP2C. After dephosphorylation reaction of phosphorylated shootin1a with PP1, PP2A or PP2C (0, 3.3, 8.3, and 16.7 ng/μl), protein mixtures were subjected to SDS-PAGE followed by immunoblotted with antibodies against pSer101, pSer249 and FLAG. Red arrowheads indicated phosphorylated shootin1a.

B. Dephosphorylation of shootin1a by PP1 in COS7 cells. Cells were transfected with vectors to express FLAG-shootin1a and myc-PP1. Cell lysates were then subjected to SDS-PAGE followed by immunoblotted with antibodies against pSer101, pSer249 and FLAG-tag. Red arrowheads indicated phosphorylated shootin1a.

C. FLAG-shootin1a was overexpressed in HEK293T cells followed by treatment for 1 hour with calyculin A. Phosphorylated FLAG-shootin1a was then purified by anti-FLAG agarose bead. The purity of FLAG-phosphorylated shootin1a was determined by CBB staining.

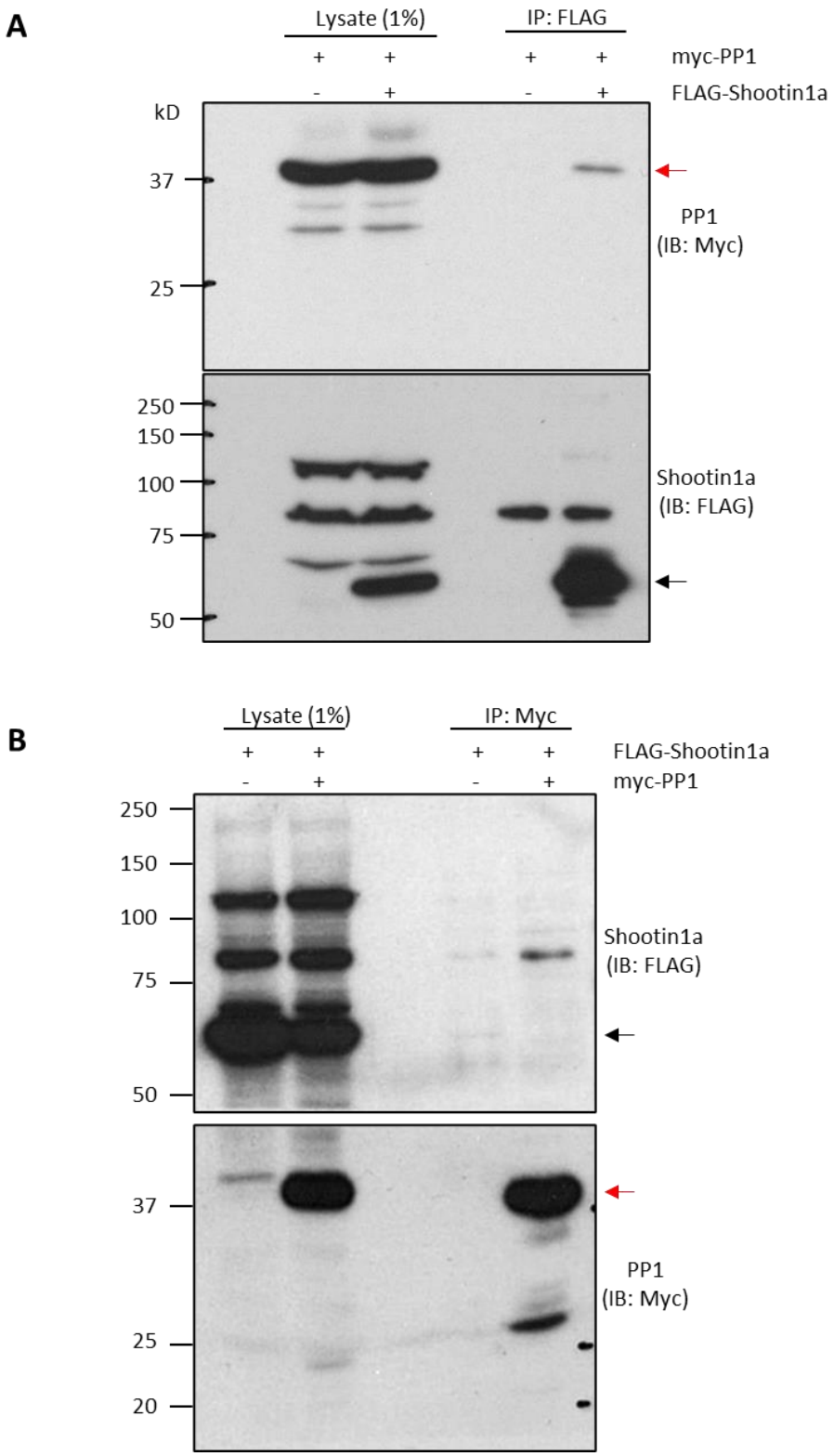

Figure S3 Coimmunoprecipitation of FLAG-shootin1a and myc-PP1 from HEK293T cells

A. Coimmunoprecipitation of FLAG-shootin1a and myc-PP1. HEK293T cells were transfected with vectors to express myc-PP1 and FLAG-shooin1a. Cell lysates were prepared and incubated with anti-FLAG antibody. The cell lysates (1%) and immunoprecipitates were immunoblotted with anti-myc or anti-FLAG antibody.

B. Reciprocal immunoprecipitation of myc-PP1 and FLAG-shootin1a. HEK293T cells were transfected with vectors to express myc-PP1 and FLAG-shooin1a. Cell lysates were prepared and incubated with anti-myc antibody. The cell lysates (1%) and immunoprecipitates were immunoblotted with anti-myc or anti-FLAG antibody. The black and red arrows indicate the FLAG-shootin1a and myc-PP1, respectively.

A

>pCMV-FLAG_Shootin1a

FLAG

DYKDDDDKRSMNSSDEEKQLQLITSLKEQAIGEYEDLRAENQKTKEKCDKIRQERDEAVKKLEEFQKISHMVIEEVNFMQ
NHLEIEKTCRESAEALATKLNKENKTLKRISMLYMAKLGPDVITEEINIDDEDSTTDTDGAAETCVSVQCQKQIKELRDQ
IVSVQEEKKILAIELENLKSKLVEVIEEVNKVKQEKTVLNSEVLEQRKVLEKCNRVSMLAVEEYEEMQVNLELEKDLRKK
AESFAQEMFIEQNKLKRQSHLLLQSSIPDQQLLKALDENAKLTQQLEEERIQHQQKVKELEEQLENETLHKEIHNLKQQL
ELLEEDKKELELKYQNSEEKARNLKHSVDELQKRVNQSENSVPPPPPPPPLPPPPPNPIRSLMSMIRKRSHPSGSGAKK
EKATQPETTEEVTDLKRQAVEEMMDRIKKGVHLRPVNQTARPKTKPESSKGCESAVDELKGILASQ

>pCMV-myc_PP1

Myc

MEQKLISEEDLSPGGSMSDSEKLNLDSIIGRLLEVQGSRPGKNVQLTENEIRGLCLKSREIFLSQPILLELEAPLKICGD
IHGQYYDLLRLFEYGGFPPESNYLFLGDYVDRGKQSLETICLLLAYKIRYPENFFLLRGNHECASINRIYGFYDECKRRY
NIKLWKTFTDCFNCLPIAAIVDEKIFCCHGGLSPDLQSMEQIRRIMRPTDVPDQGLLCDLLWSDPDKDVQGWGENDRGVS
FTFGAEVVAKFLHKHDLDLICRAHQVVEDGYEFFAKRQLVTLFSAPNYCGEFDNAGAMMSVDETLMCSFQILKPADKNKG
KYGQFSGLNPGGRPITPPRNSAKAKK

>pCAGGS-EGFP_PP1

EGFP

...**AAGITLGMDELYKRSGEF**MSDSEKLNLDSIIGRLLEVQGSRPGKNVQLTENEIRGLCLKSREIFLSQPILLELEAPLKI
CGDIHGQYYDLLRLFEYGGFPPESNYLFLGDYVDRGKQSLETICLLLAYKIRYPENFFLLRGNHECASINRIYGFYDECK
RRYNIKLWKTFTDCFNCLPIAAIVDEKIFCCHGGLSPDLQSMEQIRRIMRPTDVPDQGLLCDLLWSDPDKDVQGWGENDR
GVSFTFGAEVVAKFLHKHDLDLICRAHQVVEDGYEFFAKRQLVTLFSAPNYCGEFDNAGAMMSVDETLMCSFQILKPADK
NKGKYGQFSGLNPGGRPITPPRNSAKAKK

B

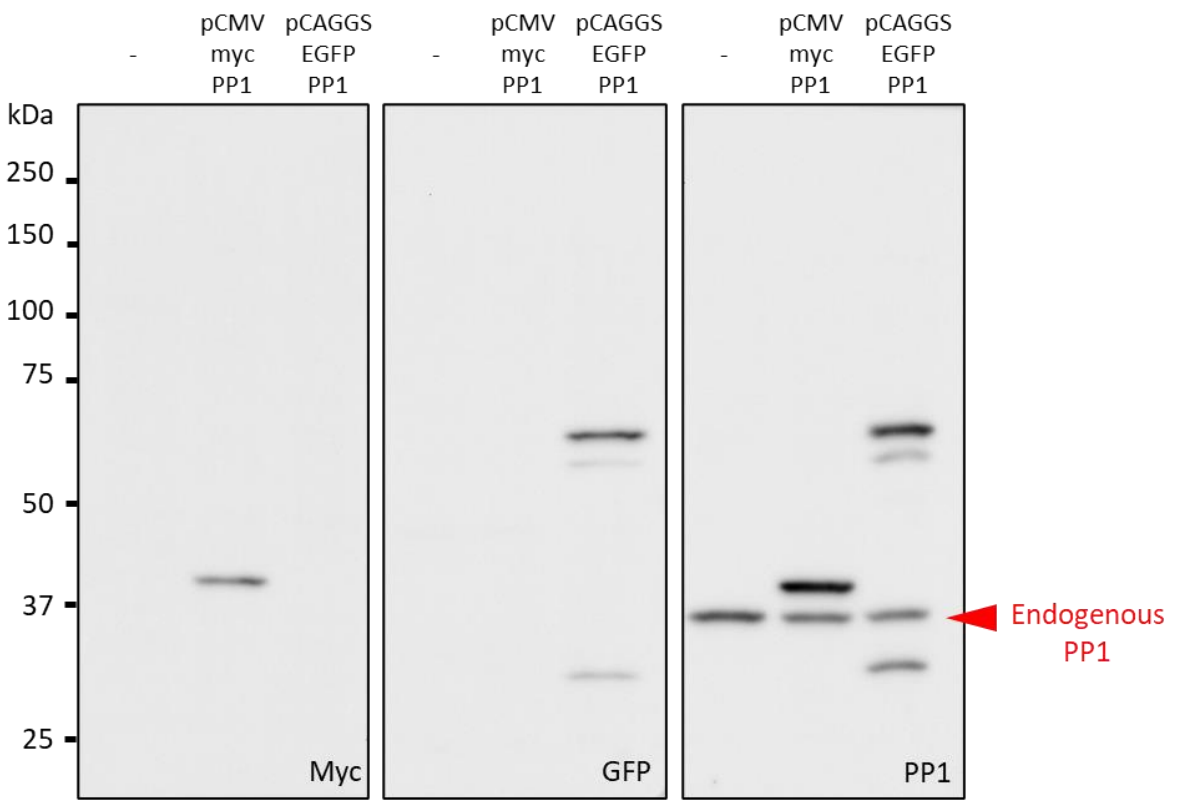

Figure S4 FLAG-shootin1a, myc-PP1 and EGFP-PP1 amino acid sequences and PP1 expression level in COS7 cells

A. Amino acid sequences of FLAG-shootin1a and myc-PP1 under CMV promoter, and EGFP-PP1 under CAGGS promoter

B. Recombinant PP1 expression level in COS7 cells. COS7 cells were transfected with plasmids to express myc-PP1 or EGFP-PP1. Cell lysates were then subjected to SDS-PAGE followed by immunoblotted with antibodies against myc-tag, GFP-tag, or PP1. Red arrowhead showed endogenous PP1 expression level.

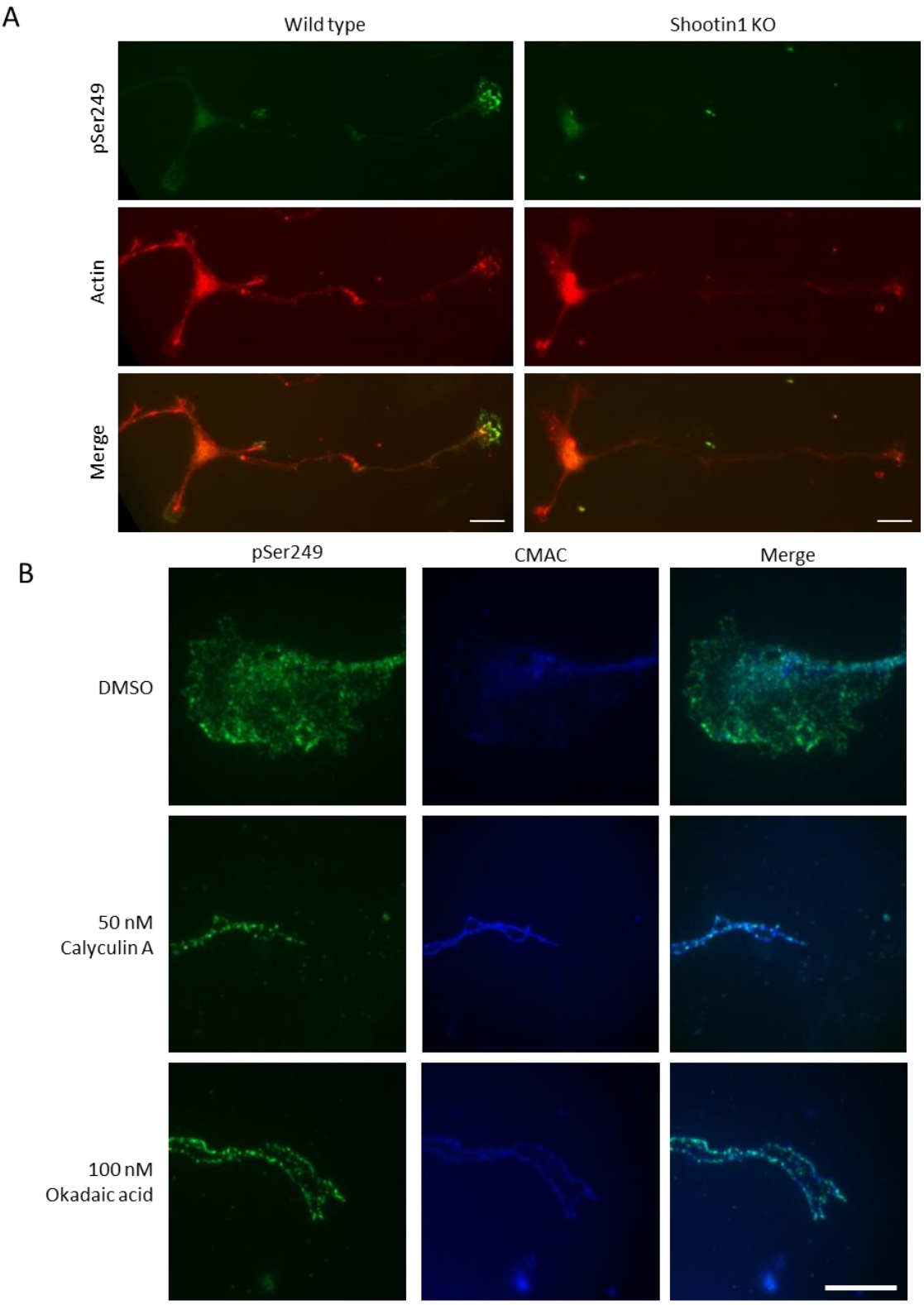

Figure S5 Specificity of phosphorylated shootin1a antibody (pSer249) and growth cone morphology after the treatment of PP1/PP2A inhibitors.

A. Fluorescence images of wild-type and shootin1 knockout neurons labeled with anti-pSer249 shootin1a (green) and anti-actin (red) antibodies. Bar: 10 μm

B. Fluorescence images of axonal growth cones after 50 nM calyculin A or 100 nM okadaic acid treatment for 30 minutes. Neurons were then fixed and immunolabeled with anti-pSer249 shootin1a (green) antibody and CMAC (blue). Bar: 10 μm

Acknowledgements

On the completion of my thesis, I would like to appreciate for the supervision throughout my five-year study from my advisor, Professor Naoyuki Inagaki. It is a pleasure to thank Professor Tomoya Tsukazaki, and Associate Professor Noriaki Sasai for the valuable comments and useful suggestions. The great suggestion becomes the important keys for developing my research outcome. My appreciation also goes to international members, Ria Fajarwati Kastian, Saranpal Singh Satinder Singh, Qiu Zhen, and Xiyao Yu, for the warm support and impressive memory. Thankfulness is also extended to all members in Laboratory of Systems Neurobiology and Medicine for their helps and for friendships that allow me to enjoy throughout my study. I would like to express my great gratitude to The Ministry of Education, Culture, Sports, Science and Technology (MEXT) scholarship for the financial support within these five years. Finally, indispensable persons and my gratefulness are my parents and all members in my family for their guidance, understanding, encouragement, endless love, and support along my long-distance education.

References

Ackerman, S.L., Kozak, L.P., Przyborski, S.A., Rund, L.A., Boyer, B.B., and Knowles, B.B. (1997). The mouse rostral cerebellar malformation gene encodes an UNC-5-like protein. Nat. 1997 3866627 *386*, 838–842.

Ardito, F., Giuliani, M., Perrone, D., Troiano, G., and Muzio, L. Lo (2017). The crucial role of protein phosphorylation in cell signalingand its use as targeted therapy (Review). Int. J. Mol. Med. *40*, 271–280.

Baba, K., Yoshida, W., Toriyama, M., Shimada, T., Manning, C.F., Saito, M., Kohno, K., Trimmer, J.S., Watanabe, R., and Inagaki, N. (2018). Gradient-reading and mechano-effector machinery for netrin-1-induced axon guidance. Elife *7*.

Barallobre, M.J., Pascual, M., Del Río, J.A., and Soriano, E. (2005). The Netrin family of guidance factors: Emphasis on Netrin-1 signalling. Brain Res. Rev. *49*, 22–47.

Bhattacharjee, N., Li, N., Keenan, T.M., and Folch, A. (2010). A neuron-benign microfluidic gradient generator for studying the response of mammalian neurons towards axon guidance factors. Integr. Biol. *2*, 669–679.

Bianchi, M., De Lucchini, S., Marin, O., Turner, D.L., Hanks, S.K., and Villa-Moruzzi, E. (2005). Regulation of FAK Ser-722 phosphorylation and kinase activity by GSK3 and PP1 during cell spreading and migration. Biochem. J. *391*, 359–370.

Bin, J.M., Han, D., Lai Wing Sun, K., Croteau, L.P., Dumontier, E., Cloutier, J.F., Kania, A., and Kennedy, T.E. (2015). Complete Loss of Netrin-1 Results in Embryonic Lethality and Severe Axon Guidance Defects without Increased Neural Cell Death. Cell Rep. *12*, 1099–1106.

Bouzigues, C., Morel, M., Triller, A., and Dahan, M. (2007). Asymmetric redistribution of GABA receptors during GABA gradient sensing by nerve growth cones analyzed by single quantum dot imaging. Proc. Natl. Acad. Sci. *104*, 11251–11256.

Boyer, N.P., McCormick, L.E., Menon, S., Urbina, F.L., and Gupton, S.L. (2020). A pair of E3 ubiquitin ligases compete to regulate filopodial dynamics and axon guidance. J. Cell Biol. *219*.

Buchser, W.J., Slepak, T.I., Gutierrez-Arenas, O., Bixby, J.L., and Lemmon, V.P.

(2010). Kinase/phosphatase overexpression reveals pathways regulating hippocampal neuron morphology. Mol. Syst. Biol. *6*, 391.

Carmody, L.C., Bauman, P.A., Bass, M.A., Mavila, N., DePaoli-Roach, A.A., and Colbran, R.J. (2004). A protein phosphatase-1γ1 isoform selectivity determinant in dendritic spine-associated neurabin. J. Biol. Chem. *279*, 21714–21723.

Cohen, P.T.W. (2002). Protein phosphatase 1 - Targeted in many directions. J. Cell Sci.

Colbran, R.J. (2004). Protein phosphatases and calcium/calmodulin-dependent protein kinase II-dependent synaptic plasticity. J. Neurosci. *24*, 8404–8409.

Das, V., and Miller, J.H. (2012). Microtubule stabilization by peloruside A and paclitaxel rescues degenerating neurons from okadaic acid-induced tau phosphorylation. Eur. J. Neurosci. *35*, 1705–1717.

Das, A.K., Helps, N.R., Cohen, P.T., and Barford, D. (1996). Crystal structure of the protein serine/threonine phosphatase 2C at 2.0 A resolution. EMBO J. *15*, 6798–6809.

Fazeli, A., Dickinson, S.L., Hermiston, M.L., Tighe, R. V., Steen, R.G., Small, C.G., Stoeckli, E.T., Keino-Masu, K., Masu, M., Rayburn, H., et al. (1997). Phenotype of mice lacking functional Deleted in colorectal cancer (Dcc) gene. Nature *386*, 796–804.

Forscher, P., and Smith, S.J. (1988). Actions of cytochalasins on the organization of actin filaments and microtubules in a neuronal growth cone. J. Cell Biol. *107*, 1505–1516.

Gungabissoon, R.A., and Bamburg, J.R. (2003). Regulation of growth cone actin dynamics by ADF/cofilin. In Journal of Histochemistry and Cytochemistry, (Histochemical Society Inc.), pp. 411–420.

Gupta, V., Ogawa, A.K., Du, X., Houk, K.N., and Armstrong, R.W. (1997). A model for binding of structurally diverse natural product inhibitors of protein phosphatases PP1 and PP2A. J. Med. Chem. *40*, 3199–3206.

Heroes, E., Lesage, B., Görnemann, J., Beullens, M., Van Meervelt, L., and Bollen, M. (2013). The PP1 binding code: A molecular-lego strategy that governs

specificity. FEBS J. *280*, 584–595.

Hoffman, A., Taleski, G., and Sontag, E. (2017). The protein serine/threonine phosphatases PP2A, PP1 and calcineurin: A triple threat in the regulation of the neuronal cytoskeleton. Mol. Cell. Neurosci. *84*, 119–131.

Hong, K., Hinck, L., Nishiyama, M., Poo, M.M., Tessier-Lavigne, M., and Stein, E. (1999). A ligand-gated association between cytoplasmic domains of UNC5 and DCC family receptors converts netrin-induced growth cone attraction to repulsion. Cell *97*, 927–941.

Inagaki, N., Ito, M., Nakano, T., and Inagaki, M. (1994). Spatiotemporal distribution of protein kinase and phosphatase activities. Trends Biochem. Sci. *19*, 448–452.

Inutsuka, A., Goda, M., and Fujiyoshi, Y. (2009). Calyculin A-induced neurite retraction is critically dependent on actomyosin activation but not on polymerization state of microtubules. Biochem. Biophys. Res. Commun. *390*, 1160–1166.

Jumper, J., Evans, R., Pritzel, A., Green, T., Figurnov, M., Ronneberger, O., Tunyasuvunakool, K., Bates, R., Žídek, A., Potapenko, A., et al. (2021). Highly accurate protein structure prediction with AlphaFold. Nat. 2021 1–11.

Kastian, R.F., Minegishi, T., Baba, K., Saneyoshi, T., Katsuno-Kambe, H., Saranpal, S., Hayashi, Y., and Inagaki, N. (2021). Shootin1a-mediated actin-adhesion coupling generates force to trigger structural plasticity of dendritic spines. Cell Rep. *35*, 109130.

Katoh, K., Hammar, K., Smith, P.J.S., and Oldenbourg, R. (1999). Birefringence imaging directly reveals architectural dynamics of filamentous actin in living growth cones. Mol. Biol. Cell *10*, 197–210.

Katsuno, H., Toriyama, M., Hosokawa, Y., Mizuno, K., Ikeda, K., Sakumura, Y., and Inagaki, N. (2015). Actin migration driven by directional assembly and disassembly of membrane-anchored actin filaments. Cell Rep. *12*, 648–660.

Keino-Masu, K., Masu, M., Hinck, L., Leonardo, E.D., Chan, S.S.Y., Culotti, J.G., and Tessier-Lavigne, M. (1996). Deleted in Colorectal Cancer (DCC) encodes a netrin receptor. Cell *87*, 175–185.

Kennedy, T.E., Serafini, T., de la Torre, J.R., Tessier-Lavigne, M., Torre, J. de la, and Tessier-Lavigne, M. (1994). Netrins are diffusible chemotropic factors for commissural axons in the embryonic spinal cord. Cell *78*, 425–435.

Killeen, M., Tong, J., Krizus, A., Steven, R., Scott, I., Pawson, T., and Culotti, J. (2002). UNC-5 Function Requires Phosphorylation of Cytoplasmic Tyrosine 482, but Its UNC-40-Independent Functions also Require a Region between the ZU-5 and Death Domains. Dev. Biol. *251*, 348–366.

Kolodkin, A.L., and Tessier-Lavigne, M. (2011). Mechanisms and molecules of neuronal wiring: A primer. Cold Spring Harb. Perspect. Biol. *3*, 1–14.

Kolpak, A.L., Jiang, J., Guo, D., Standley, C., Bellve, K., Fogarty, K., and Bao, Z.Z. (2009). Negative guidance factor-induced macropinocytosis in the growth cone plays a critical role in repulsive axon turning. J. Neurosci. *29*, 10488–10498.

Kubo, Y., Baba, K., Toriyama, M., Minegishi, T., Sugiura, T., Kozawa, S., Ikeda, K., and Inagaki, N. (2015). Shootin1–cortactin interaction mediates signal–force transduction for axon outgrowth. J. Cell Biol. *210*, 663–676.

Leung, K.M., Van Horck, F.P.G., Lin, A.C., Allison, R., Standart, N., and Holt, C.E. (2006). Asymmetrical β-actin mRNA translation in growth cones mediates attractive turning to netrin-1. Nat. Neurosci. *9*, 1247–1256.

Li, T., Chalifour, L.E., and Paudel, H.K. (2007). Phosphorylation of protein phosphatase 1 by cyclin-dependent protein kinase 5 during nerve growth factor-induced PC12 cell differentiation. J. Biol. Chem. *282*, 6619–6628.

Li, X., Wilmanns, M., Thornton, J., and Köhn, M. (2013). Elucidating Human Phosphatase-Substrate Networks. Sci. Signal. *6*, rs10–rs10.

Lin, C.H., and Forscher, P. (1993). Cytoskeletal remodeling during growth cone-target interactions. J. Cell Biol. *121*, 1369–1383.

Lowery, L.A., and Vactor, D. Van (2009). The trip of the tip: Understanding the growth cone machinery. Nat. Rev. Mol. Cell Biol. *10*, 332–343.

Malchiodi-Albedi, F., Petrucci, T.C., Picconi, B., Iosi, F., and Falchi, M. (1997). Protein phosphatase inhibitors induce modification of synapse structure and tau hyperphosphorylation in cultured rat hippocampal neurons. J. Neurosci. Res.

48, 425–438.

Menon, S., Boyer, N.P., Winkle, C.C., McClain, L.M., Hanlin, C.C., Pandey, D., Rothenfußer, S., Taylor, A.M., and Gupton, S.L. (2015). The E3 Ubiquitin Ligase TRIM9 Is a Filopodia Off Switch Required for Netrin-Dependent Axon Guidance. Dev. Cell *35*, 698–712.

Monroe, J.D., and Heathcote, R.D. (2013). Protein phosphatases regulate the growth of developing neurites. Int. J. Dev. Neurosci. *31*, 250–257.

Moorhead, G.B.G., De Wever, V., Templeton, G., and Kerk, D. (2009). Evolution of protein phosphatases in plants and animals. Biochem. J. *417*, 401–409.

Nakayama, T., Goshima, Y., Misu, Y., and Kato, T. (1999). Role of cdk5 and tau phosphorylation in heterotrimeric G protein-mediated retinal growth cone collapse. J. Neurobiol. *41*, 326–339.

Oliveira, J.M., da Cruz e Silva, C.B., Müller, T., Martins, T.S., Cova, M., da Cruz e Silva, O.A.B., and Henriques, A.G. (2017). Toward Neuroproteomics in Biological Psychiatry: A Systems Approach Unravels Okadaic Acid-Induced Alterations in the Neuronal Phosphoproteome. Omi. A J. Integr. Biol. *21*, 550–563.

Oliver, C.J., Terry-Lorenzo, R.T., Elliott, E., Bloomer, W.A.C., Li, S., Brautigan, D.L., Colbran, R.J., and Shenolikar, S. (2002). Targeting Protein Phosphatase 1 (PP1) to the Actin Cytoskeleton: the Neurabin I/PP1 Complex Regulates Cell Morphology. Mol. Cell. Biol. *22*, 4690–4701.

Robles, E., Woo, S., and Gomez, T.M. (2005). Src-dependent tyrosine phosphorylation at the tips of growth cone filopodia promotes extension. J. Neurosci. *25*, 7669–7681.

Sacco, F., Perfetto, L., Castagnoli, L., and Cesareni, G. (2012). The human phosphatase interactome: An intricate family portrait. FEBS Lett. *586*, 2732–2739.

Serafini, T., Kennedy, T.E., Gaiko, M.J., Mirzayan, C., Jessell, T.M., and Tessier-Lavigne, M. (1994). The netrins define a family of axon outgrowth-promoting proteins homologous to C. elegans UNC-6. Cell *78*, 409–424.

Serafini, T., Colamarino, S.A., Leonardo, E.D., Wang, H., Beddington, R., Skarnes, W.C., and Tessier-Lavigne, M. (1996). Netrin-1 is required for commissural axon guidance in the developing vertebrate nervous system. Cell *87*, 1001–1014.

Shao, J., and Diamond, M.I. (2012). Protein phosphatase 1 dephosphorylates profilin-1 at ser-137. PLoS One *7*.

Shi, Y. (2009). Serine/Threonine Phosphatases: Mechanism through Structure. Cell *139*, 468–484.

Shimada, T., Toriyama, M., Uemura, K., Kamiguchi, H., Sugiura, T., Watanabe, N., and Inagaki, N. (2008). Shootin1 interacts with actin retrograde flow and L1-CAM to promote axon outgrowth. J. Cell Biol. *181*, 817–829.

Sutherland, D.J., Pujic, Z., and Goodhill, G.J. (2014). Calcium signaling in axon guidance. Trends Neurosci. *37*, 424–432.

Swingle, M., Ni, L., and Honkanen, R.E. (2007). Small-molecule inhibitors of ser/thr protein phosphatases: Specificity, use and common forms of abuse. Methods Mol. Biol. *365*, 23–38.

Taylor, A.M., Menon, S., and Gupton, S.L. (2015). Passive microfluidic chamber for long-term imaging of axon guidance in response to soluble gradients. Lab Chip *15*, 2781–2789.

Toriyama, M., Shimada, T., Kim, K.B., Mitsuba, M., Nomura, E., Katsuta, K., Sakumura, Y., Roepstorff, P., and Inagaki, N. (2006). Shootin1: a protein involved in the organization of an asymmetric signal for neuronal polarization. J. Cell Biol. *175*, 147–157.

Toriyama, M., Sakumura, Y., Shimada, T., Ishii, S., and Inagaki, N. (2010). A diffusion-based neurite length-sensing mechanism involved in neuronal symmetry breaking. Mol. Syst. Biol. *6*, 394.

Toriyama, M., Kozawa, S., Sakumura, Y., and Inagaki, N. (2013). Conversion of a Signal into Forces for Axon Outgrowth through Pak1-Mediated Shootin1 Phosphorylation. Curr. Biol. *23*, 529–534.

Vereshchagina, N., Bennett, D., Szöor, B., Kirchner, J., Gross, S., Vissi, E., White-Cooper, H., and Alphey, L. (2004). The essential role of PP1β in Drosophila is to

regulate nonmuscle myosin. Mol. Biol. Cell *15*, 4395–4405.

Vicente-Manzanares, M., Ma, X., Adelstein, R.S., and Horwitz, A.R. (2009). Non-muscle myosin II takes centre stage in cell adhesion and migration. Nat. Rev. Mol. Cell Biol. *10*, 778–790.

Wang, Z., Linden, L.M., Naegeli, K.M., Ziel, J.W., Chi, Q., Hagedorn, E.J., Savage, N.S., and Sherwood, D.R. (2014). UNC-6 (netrin) stabilizes oscillatory clustering of the UNC-40 (DCC) receptor to orient polarity. J. Cell Biol. *206*, 619–633.

Wen, Z., Guirland, C., Ming, G., and Zheng, J.Q. (2004). A CaMKII/Calcineurin Switch Controls the Direction of Ca2+-Dependent Growth Cone Guidance. Neuron *43*, 835–846.

Yao, J., Sasaki, Y., Wen, Z., Bassell, G.J., and Zheng, J.Q. (2006). An essential role for ß-actin mRNA localization and translation in Ca2+-dependent growth cone guidance. Nat. Neurosci. *9*, 1265–1273.

Ziel, J.W., Hagedorn, E.J., Audhya, A., and Sherwood, D.R. (2008). UNC-6 (netrin) orients the invasive membrane of the anchor cell in C. elegans. Nat. Cell Biol. 2008 112 *11*, 183–189.